

A Paleoenvironmental analysis of Morrison Formation deposits,
Big Horn Basin, Wyoming: a multivariate approach

by

Debra S. Jennings
B.A. East Tennessee State University

Submitted to the Department of Geology
and the Faculty of the Graduate School of
The University of Kansas in partial
fulfillment of the requirements for the
degree of Master of Science
2005

Advisory Committee:

Stephen T. Hasiotis, Chair

Robert H. Goldstein

Luis A. Gonzalez

Jennifer A. Roberts

Date Submitted _____

ABSTRACT

Debra S. Jennings, M.S.
Department of Geology, May 2005
University of Kansas

The Upper Jurassic Morrison Formation, one of the most fossil-rich formations in the United States, has been well-studied in the Colorado Plateau but it has not been extensively studied in the Big Horn Basin, north-central Wyoming. Recently discovered fossiliferous deposits near Thermopolis, Wyoming, were used as a case study to test the usefulness of integrating modern and traditional methods for taphonomic and paleoenvironmental studies. A three-dimensional map of a dinosaur quarry generated from geospatial data showed two distinct bone assemblages separated by a poorly developed paleosol. Previous hypotheses of multiple feeding events by a family of allosaurids have been amended. Synthesized sedimentological, geochemical, and paleoenvironmental data from nearby Morrison deposits indicate that authigenic clays correlate to subenvironmental differences and are not laterally continuous enough to be useful in correlating strata as previous hypotheses suggest. Increase in volcanic input and corresponding changes in hydrology are recorded in three genetic stratigraphic successions. Combined geological and paleontological data show that volcanic input not climate is the dominant signature in Bighorn Basin deposits. Combined paleontological data suggests that diversity was little affected in areas distal from Late Jurassic volcanic activity in the northern part of the Morrison depositional basin. Results of this study show that multivariate methods significantly enhance taphonomic and paleoenvironmental studies, particularly those involving complex, fine-grained continental deposits.

TABLE OF CONTENTS

		<i>Page</i>
Thesis Abstract		ii
Acknowledgments		v
Dedication		vii
Chapter 1	Introduction	1
	References	2
Chapter 2	Taphonomic analysis of a dinosaur feeding site using Geographic Information Systems (GIS), Morrison Formation, southern Bighorn Basin, Wyoming, USA	
	Abstract	4
	Introduction	5
	Geologic Setting	7
	Methods	10
	Excavation techniques	10
	Mapping	10
	Microscopy	11
	Stratigraphy and Sedimentology	12
	Outcrop stratigraphy	12
	High-resolution quarry stratigraphy	13
	Paleontology	19
	Invertebrates	19
	Vertebrate fossils	19
	Vertebrate traces	25
	Geospatial distribution of vertebrate fossils	29
	Discussion	33
	Paleoenvironmental interpretations	33
	Taphonomy	35
	Conclusions	40
	References	42

Chapter 3	Paleoenvironmental and Paleoclimatic Implications of Upper Jurassic Morrison Formation Deposits, Bighorn Basin, Wyoming, USA	
	Abstract	47
	Introduction	49
	Geologic Setting	49
	Methods	52
	Stratigraphic Sections	52
	Microscopy	53
	Stratigraphy and Sedimentology	55
	Sandstone facies	59
	Siltstone facies	65
	Red mudstone facies	68
	Olive mudstone facies	72
	Greenish gray mudstone facies	75
	Greenish black siliceous facies	78
	Purple mudstone facies	80
	Black mudstone facies	81
	Greenish gray claystone facies	84
	Black claystone facies	85
	Stratigraphic and Geographic Distribution of Authigenic Minerals	88
	Clays	88
	Barite	90
	Analcime and quartz	91
	Discussion	92
	Conclusions	97
	References	102
Chapter 4	Conclusions	110

ACKNOWLEDGMENTS

Funding for this project was provided by the University of Kansas, Department of Geology August L. Selig Summer Research Award, Bighorn Basin Foundation, Clay Minerals Society, Jurassic Foundation, Paleontological Society, Panorama Society, Sigma Xi, Western Interior Paleontological Society, and a Wyoming EPScOR Summer Research Fellowship. I thank David Trexler, Robert Whittemore, and Dr. Warren Huff for their comments and critiques of the manuscript. Thanks to Frank Cole, Brandon Drake, David Lovelace, Judy Peterson, Joel Plummer, Dr. Burkhard Pohl, the staff of the Wyoming Dinosaur Center, and all volunteers who donated their time to help with data collection.

I am grateful to my committee members, Robert Goldstein, Luis Gonzalez, Steven Hasiotis, and Jennifer Roberts for their time and attention in my graduate work. I am especially indebted to Luis Gonzalez for his unwaivering support and respect and the many hours he patiently spent helping me analyze geochemical, micromorphological, and stable isotope data.

Dr. James Drever, University of Wyoming, graciously offered the use of his wet lab and provided guidance with clay XRD analysis. Dr. Dennis Eberl, Colorado USGS, Boulder, introduced me to RockJock and Mudmaster and took my clay analysis techniques to another level. Dr. Warren Huff,

University of Cincinnati, dedicated many hours over the last two years to help me hone my clay analysis skills and supported my interest in clay mineralogy and teaching.

I am also grateful to Adrian Hunt, James Steidtmann, and David Trexler who took time from their hectic schedules to ask pertinent questions, offer guidance, and point me in the right direction along the way. My long-time mentor, Robert Whittemore has remained a stalwart supporter, whose well-timed encouragement has kept me going during the hardest of times.

I will always appreciate my colleagues in the IchnoBioGeoScience Research Group and my friends and family who have stood by me. I could not have done it without you all.

DEDICATION

For Robert Whittlemore who told me, “Don’t feel the pressure, be the pressure.” It made all the difference.

CHAPTER 1: INTRODUCTION

Many paleoenvironmental studies of Morrison Formation deposits have resulted in seemingly contradictory interpretations (e.g. Stokes, 1944; Christiansen et al., 1994; Way et al., 1994; Hasiotis and Demko, 1996; Litwin et al., 1998; Peterson, 1994; Dunagan, 2000; DeCelles, 2004; Dunagan and Turner, 2004; Hasiotis, 2004; Parrish et al., 2004; Rees et al., 2004). Traditional paleoenvironmental and taphonomic research methods have tended to focus on one type of data (i.e. stratigraphy, sedimentology, geochemistry, or paleontology), but this approach has not generated consistent interpretations. Recent research has begun to employ multiple analytical methods to integrate our knowledge of Late Jurassic environments and ecology (e.g. Demko et al., 2004; Hasiotis, 2004). The goal of this study is to integrate multivariate data in taphonomic and paleoenvironmental analyses of recently discovered fossiliferous Morrison Formation deposits in southern Bighorn Basin, Wyoming.

In chapter two, Geographical Information Systems is combined with traditional mapping techniques to evaluate time-averaging of a dinosaur quarry near Thermopolis, Wyoming. Synthesis of geological, paleontological, and geospatial data is used to reconstruct quarry history.

Chapter three investigates the usefulness of integrating geochemical, paleontological, and sedimentological data to reconstruct Morrison Formation paleoenvironments in the study area. Special emphasis of this study was on evaluating the dominant influence on paleoenvironmental change during the latest Jurassic.

References

- Christiansen, E.H., Kowallis, B.J., and Barton, M.D., 1994, Temporal and spatial distribution of volcanic ash in Mesozoic rocks of the Western Interior: an alternative record of Mesozoic magmatism: *in* Caputo, M.V., Peterson, J.A., and Franczyk, K.J., eds. Mesozoic systems of the Rocky Mountain region, USA: Rocky Mountain Section SEPM, Denver, p. 73-94.
- DeCelles, P.G., 2004. Late Jurassic to Eocene evolution of the Cordilleran Thrust Belt and foreland basin system, western U.S.A.. *American Journal of Science* 304, pp. 105-168.
- Demko, T.M. and Parrish, J.T., 1998, Paleoclimatic setting of the Upper Jurassic Morrison Formation: *Modern Geology*, v. 22, p. 283-296.
- Dunagan, S.P., 2000, Lacustrine carbonates of the Morrison Formation (Upper Jurassic, Western Interior), East-central Colorado, U.S.A.: *in* Gierlowski-Kordesch, E.H. and Kelts, K.R. eds.: Lake basins through space and time: AAPG Studies in Geology, v. 46, p. 181-188.
- Dunagen, S.P. and Turner, C.E., 2004, Regional paleohydrologic and paleoclimatic settings of wetland/lacustrine depositional systems in the Morrison Formation (Upper Jurassic), Western Interior, USA: *Sedimentary Geology*, v. 167, p. 269-296.
- Hasiotis, S.T., 2004, Reconnaissance of Upper Jurassic Morrison Formation ichnofossils, Rocky Mountain Region, USA: paleoenvironmental, stratigraphic, and paleoclimatic significance of terrestrial and freshwater ichnocoenoses: *Sedimentary Geology*, v. 167, p. 177-268.
- Hasiotis, S.T. and Demko, T.M., 1996, Terrestrial and freshwater trace fossils, Upper Jurassic Morrison Formation, Colorado Plateau: *in* Morales, M., ed., *The Continental Jurassic: Museum of Northern Arizona Bulletin* 60.
- Litwin, R.J., Turner, C.E., and Peterson, F., 1998, Palynological evidence on the age of the Morrison Formation, Western Interior U.S.; *Modern Geology*, v. 22, p.297-319.
- Parrish, J.T., Peterson, F., and Turner, C.E., 2004, Jurassic “savannah” – plant taphonomy and climate of the Morrison Formation (Upper Jurassic, Western USA): *Sedimentary Geology*, v. 167, p. 137-162.

Rees, P.M., Noto, C.R., Parrish, N.J., and Parrish, J.T., 2004, Late Jurassic climates, vegetation, and dinosaur distributions: *Journal of Geology*, v. 112, p. 643-653.

Stokes, W.L., 1944, Morrison Formation and related deposits in and adjacent to the Colorado Plateau: *Bulletin of the Geological Society of America*, v. 55, p. 951-992.

Way, J.N., Malley, P.J., Furer, L.C., Suttner, L.J., Kvale, E.P., and Meyers, J.H., 1994, Correlations of the Upper Jurassic-Lower Cretaceous nonmarine and transitional Rocks in the northern Rocky Mountain foreland: *in* Caputo, M.V., Peterson, J.A., and Franczyk, K.J., eds. *Mesozoic systems of the Rocky Mountain region, USA: Rocky Mountain Section SEPM, Denver*, p. 351-364.

CHAPTER 2. TAPHONOMIC ANALYSIS OF A DINOSAUR FEEDING SITE USING GEOGRAPHIC INFORMATION SYSTEMS (GIS), MORRISON FORMATION, SOUTHERN BIGHORN BASIN, WYOMING, USA

To be submitted as:

Jennings, D.S., Hasiotis, S.T., Taphonomic analysis of a dinosaur feeding site using Geographic Information Systems (GIS), Morrison Formation, southern Bighorn Basin, Wyoming, USA. PALAIOS.

Abstract

Geospatial data collected with a Nikon Total Station from a dinosaur quarry in the upper part of the Morrison Formation in north-central Wyoming were plotted on ArcGIS ArcScene software. The resulting three-dimensional maps indicate two distinct sauropod bone assemblages with closely associated shed theropod teeth separated by a weakly developed paleosol. Consequently, previous hypotheses that all bone elements and theropod teeth in the quarry were chronologically connected are amended. Synthesis of geological and paleontological data provides evidence that a juvenile *Camarasaurus* was the center of feeding activity in a shallow-water, palustrine-lacustrine setting in the lower assemblage. The high ratio of juvenile/adult allosaurid teeth suggests one or two adults in the company of several juveniles during a scavenging event. A high incidence of theropod teeth in the upper assemblage suggests another feeding event may have occurred, but data loss from initial traditional excavation techniques precludes a more detailed interpretation. Although the Upper Jurassic Morrison Formation in the western United States yields abundant sauropod and theropod remains, few sites documenting theropod-prey interactions have been

reported. Evidence of theropod feeding activities have been difficult to establish in seemingly homogeneous continental deposits with traditional excavation techniques alone. Geographic Information Systems (GIS) is a valuable tool that allows paleontologists to establish chronostratigraphic constraints in complex continental assemblages, assess the degree of time averaging, and evaluate important geospatial patterns.

All fossils for this study were accessioned into collections at the Wyoming Dinosaur Center (WDC), Thermopolis, Wyoming. Specimen numbers are given in figure captions.

1. Introduction

The purpose of this paper is to document an *Allosaurus* feeding site in the Upper Jurassic Morrison Formation near Thermopolis, Wyoming, and to illustrate the usefulness of Geological Information Systems (GIS) for taphonomic reconstructions. Although the Morrison Formation has yielded abundant sauropod and theropod remains, few theropod-prey interactions have been documented. Tooth-damaged sauropod bones led to hypotheses of theropod feeding activities (Hunt et al., 1994; Chure, et al., 1998; Jacobsen 1998) and speculations about theropod parental behavior (Bakker, 1997). Allosaurid feeding events associated with sauropod remains have been interpreted from the Howe Quarry in northern Wyoming (Lockley et al., 1998), Como Bluff, Wyoming (Bakker, 1997), and one Upper Jurassic quarry in Thailand

(Buffetaut and Suteethorn, 1989) based on the occurrence of shed theropod teeth, sauropod remains, and dinosaur tracks within the same quarry. High incidence of theropod teeth is a characteristic connected with theropod feeding (Weishampel et al., 1990; Farlow and Holtz, 2002), but bones and teeth can accumulate over a significant amount of time in continental deposits (Martin, 1999). Without data to constrain timing of burial, chronological relationships between bones and associated teeth can be considered ambiguous.

Whether tracks, skeletal remains, and shed teeth can be related directly to a short-lived feeding event relies on high-resolution taphonomic data that delimit the degree of time averaging and distinguish subtle changes in environmental conditions. Traditional excavation and mapping techniques do not document critical, vertical relationships between fossils, particularly in homogeneous continental lithologies.

While excavating a new quarry on the Warm Springs Ranch near Thermopolis, Wyoming, in 1995, workers at the Wyoming Dinosaur Center discovered dozens of shed theropod teeth and scattered sauropod bones above a heavily trampled carbonate mudstone. Naus and Stein (1997) interpreted the site as either a predator ambush site or an *Allosaurus* den. These hypotheses were based on large numbers of shed theropod teeth, small and large tridactyl tracks, and damaged bones at the site (Naus and Stein, 1997). Excavation was suspended temporarily until geospatial data could be collected and a detailed taphonomic and sedimentary analysis could be conducted to assess the time-averaging of the assemblage and test the hypotheses.

2. Geologic setting

During the Late Jurassic-Early Cretaceous, north-central Wyoming was situated on a long, broad, floodplain (Lawton, 1994). The Nevadan orogeny allowed substantial accumulation of lacustrine and floodplain sediments in the broad, shallow sedimentary basin to the east (Lawton, 1994; Dunagan, 1998). Subsequent thrust faulting and folding resulted in lacustrine development in semi-isolated to isolated basins throughout the Western Interior (Carson, 1998; Dunagan, 1998) as island-arc terranes were accreted to the northwestern continental margin between the Middle Jurassic and Middle Cretaceous (DeCelles, 2004). Volcanism and uplift along the collision belt increased sedimentation rates during the Kimmeridgian and Tithonian (Brenner and Peterson 1994) as significant amounts of volcanic debris and ash were generated from the Transcontinental Arc to the west and deposited eastward and northeastward across the Western Interior (Suttner, 1969; Peterson, 1972; Santos and Peterson, 1986; Johnson, 1991; Dunagan, 1998; DeCelles, 2004).

The subject of this study, the Something Interesting (SI) quarry, is located approximately 2.5 kilometers southeast of Thermopolis, in north-central Wyoming, at the southernmost extent of the Bighorn Basin (Fig. 1A). A semi-temporary shelter covers the current excavation surface of 4 x 15 m. A metal walkway was built across the quarry to protect a trampled surface from any unnecessary traffic and to allow access for Wyoming Dinosaur Center museum tours.

Outcrops in the study area trend east-northeast, dipping 6° N. The Morrison Formation is approximately 60 m thick in most local stratigraphic sections and is bounded by disconformable contacts with the Upper Jurassic Sundance Formation at the base and the Lower Cretaceous Cloverly Formation at the top. The contact between the Morrison and the Sundance Formation is identified as the contact between a quartz-rich, trough-crossbedded sandstone unit lying directly above a green, glauconitic, bioclast-rich sandstone unit. The Morrison-Cloverly contact is highly erosional with large, trough-crossbedded, chert-pebble conglomerate of the Cloverly overlying greenish gray or black, organic-rich claystone of the Morrison (Fig. 1B).

3. Methods

3.1 Excavation techniques

Awls, oyster knives, and dental picks were used to pry apart rocks, working from the top of the deposits down to the basal carbonate mudstone. Each rock was examined carefully as it was disaggregated to ensure that as many teeth, gastroliths, invertebrate fossils, and skeletal elements as possible were documented *in situ*. The use of rock hammers was limited to splitting indurated rocks into pieces small enough to ensure that no small constituents were overlooked. Hand lenses were used to look for microfossils.

3.2 Mapping

All specimens in the quarry were initially mapped on grid paper using traditional methods. A meter grid was established and each element was measured with a Brunton compass and tape measure and then drawn on a master map.

Plan-view maps of the quarry were generated from a one-meter grid system marked off with string and compass. Digital photographs of each grid were used to correct preliminary quarry maps and confirm the exact location of each element. The strike and dip of each specimen was measured with a Brunton compass.

A Nikon Total Station was used to collect x-y-z data on each element from reference points in the quarry. Two measurements were taken along the long axis of bones longer than six centimeters. Teeth and small fragments were documented as single measurements. All x-y-z data were entered into a database file and imported into ArcGIS ArcScene to create a three-dimensional map. A corrected map of the lower bone assemblage was generated using data from the three-dimensional map.

Eight stratigraphic sections of the entire Morrison Formation were measured with a precision Jacob's staff and described in the area to put the quarry in stratigraphic context. A cross section was generated from three high-resolution stratigraphic sections measured along the length of the quarry.

3.3 Microscopy

Thin sections of carbonate mudstone and mudstone units, bone material-matrix interface, and concretions found in the quarry were examined for pedogenic microfabric, microfossils, and other mineralogical characteristics. Samples of

mudstones, carbonates, and nodules systematically collected every 5 cm throughout the sequence were analyzed with X-ray diffraction (XRD) to identify authigenic mineral composition. The less than 0.5 μ m size fraction of the clay minerals was separated from samples by standard centrifugation methods. Clay samples were then saturated with 10% KCl and MgCl (Moore and Reynolds, 1997), mounted on glass slides using Drever's Millipore method (1973), and glycolated for two days. Randomly oriented powdered samples of nodules associated with bone material and clay samples were analyzed by powder XRD on a SCINTAG XDS 2000 with CuK α radiation. Scans were evaluated with methods described in Moore and Reynolds (1997).

4. Stratigraphy and Sedimentology

4.1 Outcrop stratigraphy

Although deposits are laterally variable, stratigraphic sections exhibit three basic lithofacies associations (Fig. 1B). The lower 45 m are composed of interbedded quartz-rich, fine-grained sandstone and mudstone. The sandstone units are trough cross-stratified with few ripple cross laminations. Three meter-scale, white sandstone units at the top of this sequence show small-scale cross beds and ripple marks separated by thin centimeter-scale shale layers.

The interbedded sandstone-mudstone facies is overlain by 12 m of interbedded carbonate mudstone and mudstone. Carbonate units thin and thicken, and in some places appear nodular, similar to palustrine-lacustrine strata described by Freytag and Plaziat (1982) and Wright and Platt (1995). Micritic concretions from 1mm – 30 mm

in diameter are well-distributed throughout the mudstone. Up section, carbonate mudstone units thicken and mudstone units thin until reaching a 1 m thick nodular unit. The interbedded carbonate mudstone-mudstone succession has a lenticular geometry, thinning to the north and south along the outcrop.

Eight nearly complete, dinosaur skeletons have been discovered in the carbonate mudstone-mudstone facies. Most quarries yield well-preserved, articulated camarasaurid, apatosaurid, or diplodocid sauropod material. SI is located approximately 12 m below the Morrison-Cloverly contact.

The top three m of the Morrison are composed of purple (5P4/2), clay-rich mudstone with greenish gray (5GY6/1-5GY4/1) mottles, overlain by approximately one meter of organic-rich claystone. Dense globular concretions in the purple mudstone range in size from 2-24 cm in diameter. These concretions appear to be nucleated around organic material or are associated with large conical-shaped steinkerns. Topping the sequence is a structureless, black, organic-rich claystone.

4.2 High-resolution quarry stratigraphy

Bone-bearing units vary in thickness from 30-80 cm vertically, with the thickest deposits near the middle of the quarry (Fig. 2). Although only two units are readily apparent, geological and paleontological data revealed two more layers.

Unit one is composed of a 40 cm thick, heavily trampled, light gray, (N6) carbonate mudstone (Fig. 2). Most tracks extend 20-40 cm below the surface. The matrix is dominantly Ca-Mg smectite with a minor component of bioclasts and volcanic air-fall ash material including zircons, plagioclase, and minor amounts of

olivine. Darker gray, clay-rich (5GY4/1) mudstone infills the lowest levels of undulations in the trampled surface.

Barite nodules are closely packed around bone material in unit one (Fig. 3A). No barite nodules have been found in any other units in the quarry or more than 1 cm away from bone elements. Overlying mudstone is compacted preferentially around the barite nodules, suggesting they formed in the sediments prior to significant burial. The nodules have a granular texture with sparry calcite in dilational fractures (Fig. 3B). Bone material in this unit is permineralized with calcite and shows no signs of stress from compaction (Fig. 3C).

Unit two is composed of a 20-50 cm greenish gray (5GY5/1), silty mudstone that is noncalcareous except for sparse micritic calcite nodules with poorly defined boundaries and micritic coatings on unidentifiable bone fragments. Bone fragments 0.5-6 cm in size are larger at the base of the unit, becoming smaller and less well preserved toward the top of the unit. Poorly preserved bone fragments appear brecciated with sparry calcite infilling remnant cells. The micritic matrix fills pores between brecciated bone and collapsed cells (Fig. 3D). Minor dark gray clay intraclasts are found in the lower six centimeters of the unit. Vermiculite-illite mixed-layer clays dominate the mudstone. Desiccation cracks with associated slickensides extend to 5-10 cm above unit 1 (Fig. 3E). Vertical to sub-vertical burrows extend from the top of unit two near the southern end of the quarry (Fig. 3F).

Unit three is a trampled, light gray carbonate (N6) mudstone 10-20 cm in thickness. Clay composition in this unit is dominantly Fe-rich smectite. One tridactyl

track was found directly underneath an undulation in this unit at the top of unit two (Fig. 4A-D). Darker greenish gray claystone (5GY4/1) occurs in carbonate mudstone that together infill the track (Fig. 4B). Loading was restricted to approximately 4 cm directly underneath the track and disruption was limited to 6 cm laterally adjacent to the track (Fig. 4B). Pullups in this track (Fig. 4 D) and morphology of the trampled carbonate mudstone (Fig. 4A, B) suggest that it was made when the carbonate mud and overlying clay sediments were saturated to the top of unit two. This track delineates a disconformable surface between unit two and unit three that would otherwise appear conformable. Ten cm of black claystone (N2) infills unit three. Near undulations in unit three there is convoluted bedding. Some small stringers of siltstone occur across the quarry.

5. Paleontology

5.1 Invertebrates

Thin sections of the basal carbonate mudstone show bioclasts of ostracodes, bivalves, and gastropods (Fig. 5A). Pockets of ostracodes and choncostracans were also found associated with convolute bedding in the upper claystone of unit four (Fig. 5B, C). No invertebrates have been documented in unit two, however, occasional vertical to subvertical calcite-lined burrows are present in the upper 10 cm (Fig. 3E).

5.2 Vertebrate fossils

A total of 101 theropod teeth ranging from 2-50 mm in length (Fig. 5D) were discovered in the quarry; 53 were removed during initial excavations and 48 were

collected with associated geospatial data. Vertebrae of three genera of sauropods were field identified as *Camarasaurus*, *Appatosaurus*, and *Diplodocus* during initial excavations. Sauropod material includes pes claws from 3-10 cm in length, rib fragments, one whole rib, caudal, sacral, and cervical vertebrae, pubic bones, scapulae, limb elements, and teeth with root material attached. Most of the sauropod material is disarticulated but there are three distinct groups of articulated remains associated with theropod teeth. Specimens have been permineralized with calcite and show some variability in preservation. Bones found in carbonate mudstone show no indication of alteration from subaerial exposure in spite of trampling and tooth damage. Bone material excavated from unit two is fragmented, worn, and weathered.

The largest group of bones is located at the southwest end of the quarry in a depression in unit one (Fig. 6A). The morphology of closely associated caudal vertebrae and chevrons indicate the specimen is a juvenile *Camarasaurus*. Although the bones are not articulated, there is a predictable anterior to posterior distribution of material with ilium, ischium, and caudal bones to the north, and rib fragments and skull material to the south. Twenty-three caudal vertebrae are distributed at the north end of this assemblage. No evidence of alteration from subaerial exposure of the bone material has been documented.

Two scapulae, a pubis, and half a humerus in the basal carbonate mudstone have V-shaped grooves along damaged edges where large pieces of bone are missing (Fig. 6B). The pubis is approximately one meter to the south of the ilium and ischium bones. The scapulae were separated by 1.5 m. Sacral vertebrae were displaced nearly

two m to the east of the illium and ischium and limb bones were scattered away from the main bone assemblage by 0.5-2 m. Also associated with the sacral vertebrae are several large fragments of a radius.

Most theropod teeth are within 3 centimeters of rib fragments and large bones, with the heaviest concentration between the pectoral and pelvic elements. Theropod tooth morphology and serration counts of 12-18/5 mm are consistent with allosaurid teeth (Farlow et al., 1991). The ratio of juvenile to adult theropod teeth is approximately 2:1. Thirteen juvenile *Camarasaurus* teeth were scattered among bones found in unit one. Most were lying directly on the carbonate mudstone surface.

Five caudal vertebrae were vertically impressed into the carbonate mudstone (Fig. 7A). Trampling in unit one abruptly ends in the middle of the assemblage around a definite depression where most of the rib material was found (See fig. 6A).

Also associated with caudal vertebrae and broken ischium and illium bones were 14 polished quartz clasts from 1– 13 cm in diameter (Fig. 7B). All but three of these stones were suspended in the clay-rich mudstone immediately above unit one and were restricted to 0.025 m³ of rock between caudal vertebrae and broken pelvic bones.

5.3 Vertebrate traces

Dinosaur tracks occur at three levels in unit one. Most tracks extend to 30-40 cm below the trampled surface (Fig. 8A), obliterating any discernable track morphology. The morphology of most shallow tracks is consistent with juvenile sauropod tracks. Bordering the caudal vertebrae at the northwest end of the quarry are at least five well-preserved pentadactyl tracks that crosscut the deeper tracks and extend only 13-15 cm

into the carbonate mudstone. The best-preserved track is 35 cm wide x 41 cm long x 9 cm deep and is complete with five digits and a heel pad impression (Fig. 8B). The carbonate mudstone is pushed up around the front of each of these tracks, indicating an east-west sense of movement. No clear trackway is apparent. In the middle of the quarry two sauropod tracks over 40 cm in diameter also crosscut the deeper tracks but only extend 5 centimeters into the carbonate mudstone (Fig. 8A). Two small, flattened, caudal vertebrae were found in the base of the tracks (Fig. 8A).

Isolated theropod tracks are found around the depression in the carbonate mudstone of unit one. At the south end of the depression in unit one, there is one distinct tridactyl track 62 cm long and 42 cm wide associated with fragments of skull material. Immediately adjacent to this track is three V-shaped grooves with claw impressions at one end. The grooves are approximately 5 cm wide and infilled with dark gray claystone, becoming deeper toward the claw impressions. The total spread is 43 cm at mid point and there is about 20 cm between each groove at the widest end (Fig. 9A, B). Similar grooves flank the *Camarasaurus* remains on the east side of the depression. Claystone is impressed into these grooves and is much finer grained than the overlying unit. One large groove correlates with a tooth-damaged humerus bone located at the south end of the quarry.

5.4 Geospatial distribution of vertebrate fossils

Three-dimensional maps generated with ArcGIS ArcScene show two distinct genetic assemblages of sauropod bones and associated theropod teeth (Fig. 10A). The lower assemblage is the most extensive in which 25 theropod teeth are grouped in a

depression with associated rib fragments and pectoral elements in unit one and the lower part of unit two. The assemblage thickens in the region of the depression and spans approximately 13 m laterally. Twelve theropod teeth are associated with the scapula and caudal vertebrae at either end. The relationship of bones, teeth, and gastroliths can be examined by rotating the three-dimensional map. A view of the highest concentration of bones and teeth indicate that the bone fragments, gastroliths, and theropod teeth are distributed within an area of less than 4.5 m³ (Fig. 10B). Figure 11A is the map generated with traditional methods. Figure 11B shows the corrected map of the lower bone assemblage produced from the three-dimensional data.

The second and smallest assemblage is in unit three at the north end of the quarry. Fragmentary bones and theropod teeth are clustered along a three meter line, trending in a general north-south direction (Fig. 10A). No large bones or vertebrae are associated with this assemblage.

6. Discussion

6.1 Paleoenvironmental interpretations

Ostracodes and conchostracans in the fine-grained mudstone and claystone of units one, three, and four indicate a shallow, neutral to alkaline lacustrine setting for the SI quarry (Lucas and Kirkland, 1998; Schudack et al., 1998; Stankiewicz, 1998).

Modern ostracodes tolerate a wide range of water chemistry and fluctuating environments, but modern conchonstracans prefer small, shallow, ephemeral water bodies that range in temperature from 4-30° C with a pH range of 7 to 9.7 (Frank, 1988). Based on comparison modern analogues it is reasonable to expect that Morrison ostracodes and conchonstracans likely indicate fluctuating water chemistry and alternating wet and dry conditions in transitional areas surrounding shallow water environments. Although chitinous organisms such as conchonstracans were once thought to be very delicate with a low preservation potential, Smith (2000) documented a larger preservation potential of chitin-producing organisms in palustrine-lacustrine deposits near ephemeral lakes. Interlayered carbonate mudstone-mudstone units were deposited rapidly in marginal, shallow-water environments with shorelines fluctuating in response to alternating wet-dry episodes (Platt, 1989; Wright and Platt, 1995; Dunagen and Turner, 2004). During wet periods, submersion of low-lying areas allowed accumulation of carbonate mud and recolonization of freshwater invertebrates.

Burrows and micritic calcite-coated bone fragments in unit two show that during regressive phases, poorly developed paleosols formed in transitional areas as plants and animals moved into previously submerged areas (Freytet and Plaziat, 1982).

Sporadic influx of surface water and slight fluctuations in groundwater resulted in shrink-swell features such as slickensides and deep desiccation cracks in sediments dominated by swelling clays (Freytet and Plaziat, 1982). Ca-Mg smectite in the palustrine carbonate mudstones suggests a higher alkalinity (Chamley, 1989; Hillier, 1995). Vermiculite-illite mixed layer clays, often found in better-drained, poorly-developed soils, indicate that smectite-rich sediments resulting from alteration of fine-grained volcanic ash continued to be modified in a marginal, alkaline, aqueous environment (Velde, 1995; Moore and Reynolds, 1997). Pedogenic processes, resulting in weathered and fragmented bones, modified bones previously buried in submerged sediments. Continued wetting and drying caused micritic calcite coatings of grains and larger clasts in unit two in a process similar to that described by Nahon (1991). Remnant cells of poorly preserved and weathered bone material infilled with sparry calcite in unit two suggest the bone fragments were permineralized and pedogenically reworked.

Barite concretions are not well documented in continental deposits, however, similar concretions have been reported from modern deep-water marine sediments and barite precipitation has been documented in a few alkaline-saline lakes (Lyons et al., 1994; Breheret and Brumsack, 2000; Smith et al., 2004). Barite precipitation is a process that almost always occurs in environments where separate barium-rich and sulfate-rich fluids converge (Hanor, 2000). Granular texture is associated with low temperature precipitation of barite (Hanor, 2000). Brumsack (1986) suggested that low temperature barite precipitation is closely associated with decaying organic matter.

High concentrations of barium have been documented in clay-rich sediments of volcanically influenced wetland systems (Ashley and Driese, 2000). In this setting, the oxidation of thiol from residual decaying flesh of the juvenile *Camarasaurus* would have provided the necessary sulfate for barite precipitation around bones buried in shallow water.

Synthesis of geologic data indicates that the interlayered carbonate mudstone-mudstone units at SI were deposited during alternating wet and dry conditions. Although the exact time required for these deposits to accumulate is impossible to determine, it is reasonable to suggest a decadal scale for these fluctuations in hydrology based on pedogenic and sedimentological features.

6.2 *Taphonomy*

Two distinct assemblages of sauropod bone material associated with high numbers of shed theropod teeth indicate that two feeding events occurred at distinctly different times. The upper assemblage is fragmentary and incomplete, but the close association of shed theropod teeth and bone material suggests it was part of another feeding event. Unfortunately, it is likely that many elements from the upper assemblage were removed without corresponding geospatial data during initial quarry work, making it impossible to document a scatter pattern from this level.

The lower assemblage reveals a high juvenile-adult ratio of allosaurid teeth associated with tooth-damaged juvenile *Camarasaurus* remains. Presuming a slow rate of theropod tooth replacement suggested by Farlow et al. (1991), this ratio likely

corresponds to the number of individuals present at the time of the feeding event. Consequently, barring ontogenetic differences in tooth loss, the number of juvenile allosaurids appears to have been at least twice that of the number of adults.

Distribution of allosaurid teeth in unit one indicates that most of the feeding activity was centered in the anal and gastro-intestinal regions, an area that would offer the easiest access to visceral elements (Weigelt, 1989). Scavengers and predators often begin feeding by rupturing the body cavity near the pelvic girdle (Weigelt, 1989; Wings, 2004). Associated large polished stones found suspended in clay-rich mudstone near the body cavity are difficult to explain in a sedimentary context. The velocity of flowing water necessary to move quartz clasts up to 3 centimeters in diameter is 200 cm/s in a low gradient system, a velocity that would move large sauropod bones and clay-sized sediments (Reinck and Singh, 1980). Gastroliths are also scattered when a decaying carcass drifts in water currents (Wings, 2004). The preservation of gastroliths is highest in autochthonous skeletons buried in quiet, shallow water settings (Wings, 2004). The most parsimonious explanation of such large clasts suspended in clay-rich mudstone in close association with pectoral and pelvic girdle elements is that these stones are gastroliths (Sanders et al., 2001; Wings, 2004).

The occurrence of 14 gastroliths clustered near pelvic elements suggests that the body cavity was protected from normal surficial degradational processes (Wings, 2004). The juvenile *Camarasaurus* carcass was partially submerged in less than a meter of water, preventing the gastroliths from being separated more than a few centimeters

from the gastric area (Wings, 2004). Remains were subsequently buried in this shallow water setting with no subaerial exposure.

Grooves around the body, interpreted as claw marks, suggest that overlying clay-rich sediments were pushed in to the underlying cohesive substrate under saturated conditions. Orientation of V-shaped grooves along the edges of the pubic bone and scapula indicate that these elements were dislocated past one another during the feeding activity. Since large portions of the juvenile *Camarasaurus* were dislodged and removed from the central body elements and caudal vertebrae were vertically trampled into the carbonate mud, the body may have been already in a state of decay when the allosaurids began feeding. The body of the juvenile sauropod lying in shallow water prevented trampling of the mud under the body, but did not preclude trampling around the periphery. After the feeding event, remaining bones in shallow water were protected from weathering and quickly buried and subsequently permineralized.

Tracks in the basal carbonate mudstone infilled with greenish gray mudstone are strikingly similar to tracks documented in palustrine-lacustrine deposits adjacent to alkaline lakes in Tanzania (Ashley and Liutkus, 2002). Multiple levels of tracks indicate a high traffic near-shore area during a period of drying, followed by flooding that subsequently buried and preserved the tracks.

Synthesized data supports that a juvenile *Camarasaurus* was scavenged in a near-shore, shallow, aqueous setting (Fig. 12 A, B). Feeding activity was centered in the anal area and body cavity. Limb material was highly tooth-damaged and scattered away from the body, indicating a normal scatter pattern for feeding activity (Weigelt,

1989). There are not sufficient data to document how the juvenile *Camarasaurus* died, but since at least 40 percent of the individual is present and associated with gastroliths, it is likely that it was not transported by the allosaurids that fed on it. The occurrence of gastroliths in clay-rich sediments and in close association with rib fragments suggests a relatively quiet water system. Moderately alkaline water contributed to barite precipitation within a few centimeters of the sediment-water interface during microbial decay of residual flesh (Fig. 12C).

The feeding events were separated by enough time for a weak paleosol to develop (Fig. 12D). How much time is represented by this unit is indeterminable, however, it is reasonable to suggest that it was enough to separate the feeding events by as much as a decade. Subsequently, subaqueous conditions returned allowing accumulation of another trampled carbonate mud and bone assemblage (Fig. 12E).

Results of this study show that there are no data to support previous hypotheses of recurrent feeding activity in the area by the same group of individuals. Geological and geospatial data that restrict chronological association between the two assemblages indicates that although there may have been two feeding events, recurrent feeding by one group of individuals is not likely. Shallow water conditions supported by the paleoenvironmental reconstruction of the quarry rule out the possibility that the area was the site of an Allosaurid den. Indications that the *Camarasaurus* was already in latter stages of decay before the Allosaurids began feeding suggest that a scavenging event is more likely than ambush predatory activity.

7. Conclusions

The abundance of well-preserved sauropod and theropod dinosaurs in the Morrison Formation contrasts with the paucity of documented feeding sites. This is likely a function of collection bias as most excavation foci have been on harvesting the fossils and not on collecting independent geologic and three-dimensional geospatial data. Apparent homogeneous continental deposits also make it difficult to assess accurately the time averaging of such complex assemblages as feeding sites. Results presented in this paper show that GIS is a useful tool that permits paleontologists to assess time averaging of vertebrate assemblages and provide tighter chronological constraints on paleoenvironmental reconstructions. As a result of this study we offer the following recommendations:

- A comprehensive approach should be used with continental assemblages, particularly those found in clay-rich deposits. It is crucial that high-resolution geological data and paleontological data be collected at every quarry.
- Collection and assessment of all elements for tooth damage, insect damage, pedogenic, and diagenetic data should be incorporated into site management plans for all dinosaur quarries.
- Geospatial data should be collected and used to generate three-dimensional maps with correlative geologic data at all sites, especially where there is a high incidence of shed theropod teeth.

References

- Ashley, G.M., Driese, S.G., 2000. Paleopedology and paleohydrology of a volcanoclastic paleosol interval: implications for early Pleistocene stratigraphy and paleoclimate record, Olduvai Gorge, Tanzania, 70, pp. 1065-1080.
- Ashley, G.M., Liutkus, C.M., 2002. Tracks, trails and trampling by large vertebrates in a rift valley paleo-wetland, lowermost bed II, Olduvai Gorge, Tanzania. *Ichnos*, 9, pp. 23-32.
- Babcock, L.E., Rode, A.L., Leslie, S.A., Ford, L.A., Polak, K., Becker, L. 2004. Microbially mediated precipitation of carbonates and exceptional preservation of Fossils in the Kirkpatrick basalt (Jurassic) of Antarctica. *Geological Society of America Abstracts with Programs*, 36, 5, pp. 475.
- Bakker, R.T., 1997. Raptor family values: *Allosaur* parents brought giant carcasses into their lair to feed their young. In: Wolberg, D.L., Sump, E., Rosenberg, G.D., *Dinofest International, Proceedings of a Symposium sponsored by Arizona State University*, pp. 51-63.
- Breheret, J.G., Brumsack, H.J., 2000. Barite concretions as evidence of pauses in sedimentation in the Marnes Bleues Formation of the Vocontial Basin (SE France). *Sedimentary Geology*, 130, pp 205-228.
- Brenner, R.L., Peterson, J.A., 1994. Jurassic sedimentary history of the northwestern portion of the western interior seaway, USA. In: Caputo, M.V., Peterson, J.A., and Franczyk, K.J., (eds.), *Mesozoic systems of the Rocky Mountain region, USA: Rocky Mountain Section, Society of Economic Paleontologists and Mineralogists, Special Publication*, pp. 217-232.
- Brumsack, H.J., 1986. The inorganic geochemistry of Cretaceous black shales (DSDP Leg 41) in comparison to modern upwelling sediments from the Gulf of California. *Geological Society of America Special Publication*, 21, pp. 447-462.
- Buffetaut, E., Suteethorn, V., 1989. A sauropod skeleton associated with theropod teeth in the Upper Jurassic of Thailand: remarks on the taphonomic and palaeoecological significance of such associations. *Palaeogeography, Palaeoclimatology, Palaeoecology*, 73, pp. 77-83.

- Carson, C.J., 1998. The structural and stratigraphic framework of the Warm Springs Ranch area, Hot Springs County, Wyoming. MS thesis, Oklahoma State University, Stillwater Oklahoma, pp 90.
- Chamley, H., 1989. *Clay Sedimentology*: Springer-Verlag, New York, 623 p.
- Chure, D.J., Fiorillo, A.R., Jacobsen, A.R., 1998. Prey bone utilization by predatory dinosaurs in the Late Jurassic of North America, with comments on prey bone use by dinosaurs throughout the Mesozoic. *Gaia*, 15, pp.227-232.
- DeCelles, P.G., 2004. Late Jurassic to Eocene evolution of the Cordilleran Thrust Belt and foreland basin system, western U.S.A.. *American Journal of Science* 304, pp. 105-168.
- Drever, J.I., 1973. The preparation of oriented clay mineral specimens for X-ray Diffraction analysis by a filter-membrane peel technique. *American Mineralogist*, 58, pp. 553-554.
- Dunagan, S.P., 1998. Lacustrine and Palustrine Carbonates from the Morrison (Upper Jurassic) East-central Colorado, USA: Implications for Depositional Patterns, Paleoecology, Paleohydrology, and Paleoclimatology Dissertation University of Tennessee, Knoxville.
- Dunagan, S.P., Turner, C.E., 2004. Regional paleohydrologic and paleohydrologic setting of wetland/lacustrine depositional systems in Morrison Formation (Upper Jurassic), Western Interior, USA. *Sedimentary Geology*, 167, pp. 269-296.
- Farlow, J.O., Brinkman, D.L., Abler, W.L., Currie, P.J. 1991. Size, shape, and serration density of theropod dinosaur lateral teeth. *Modern Geology*, 16, pp. 161-198.
- Farlow, J.O., Holtz, Jr., T.R., 2002. The fossil record of predation in dinosaurs. *Paleontological Society Papers*, 8, pp. 251-265.
- Frank, P.W., 1988. Conchostraca. *Palaeogeography, Palaeoclimatology, Palaeoecology*, 62, pp. 399-403.
- Freytet, P. and Plaziat, J.C., 1982. Continental carbonate sedimentation and pedogenesis -- Late Cretaceous and Early Tertiary of southern France. In: Purser, B.H. ed., *Contributions to Sedimentology* 12, E. Schweizerbart'sche Verlagsbuchhandlung, Stuttgart, pp. 213.

- Hanor, J.S., 2000. Barite-celestine geochemistry and environments of formation, In: Alpers, C.N., Jambor, J.L., and Nordstrom, D.K., eds., Sulfate Minerals: crystallography, geochemistry, and environmental significance: Reviews in Mineralogy and Geochemistry: Washington D.C., Mineralogical Society of America, p. 193-275.
- Hillier, S., 1995, Erosion, sedimentation, and sedimentary origin of clays, In: Velde, B., ed., Origin and Mineralogy of Clays: clays and the environment: Springer-Verlag, New York, p. 162-219.
- Hunt, A.P., Meyer, C.A., Lockley, M.G., Lucas, S.G., 1994. Archaeology, toothmarks and sauropod dinosaur taphonomy. *Gaia*, 10, pp. 225-231.
- Jacobsen, A.R., 1998. Feeding behavior of carnivorous dinosaurs as determined by tooth marks on dinosaur bones. *Historical Biology*, 13, pp. 17-26.
- Johnson, J. 1991. Stratigraphy, sedimentology, and depositional environments of the Upper Jurassic Morrison Formation, Colorado Front Range, PhD Dissertation, University of Nebraska, Lincoln, pp. 171.
- Lawton, T.F. 1994. Tectonic setting of Mesozoic sedimentary basins, Rocky Mountain region, United States. In: Caputo, M.V., Peterson, J.A., and Franczyk, K.J., (eds.), Mesozoic systems of the Rocky Mountain region, USA: Rocky Mountain Section, Society of Economic Paleontologists and Mineralogists, Special Publication, p. 1-25.
- Lockley, M.G., Meyer, C.A., Siber, H.J., Pabst, B., 1998. Theropod tracks from the Howe quarry, Morrison Formation, Wyoming. *Modern Geology*, 23, pp. 309-316.
- Lucas, S.G., Kirkland, J.I., 1998. Preliminary report on conchostraca from the Upper Jurassic Morrison Formation, western United States. *Modern Geology*, 22, pp. 4415-422.
- Lyons, W.B., Hines, M.E., Last, W.M, Lent, R.M., 1994. Sulfate reduction rates in microbial mat sediments of differing chemistries: implications for organic carbon preservation in saline lakes. *Sedimentology and Geochemistry of Modern and Ancient Saline Lakes*, SEPM Special publication, 50, pp.13-20.

- Martin, R.E., 1999. Taphonomy: A process approach, Cambridge University Press, pp. 508.
- Moore, R.C. and Reynolds, D.M., 1997. X-ray diffraction and the identification and analysis of clay minerals, Oxford University Press, pp. 378.
- Nahon, D.B., 1991. Introduction to the petrology of soils and chemical weathering. John Wiley and Sons, New York, pp. 3113.
- Naus, M.T., Stein, W.W., 1997. On Behavior of the Late Jurassic Carnivores. Report: Big Horn Basin Foundation / Wyoming Dinosaur Center, pp. 2.
- Peterson, J.A., 1972. Jurassic System. In: Mallory, W.W. Ed. Geologic Atlas of the Rocky Mountain Region, Rocky Mountain Association of Geologists, Denver, Colorado, pp.331.
- Platt, N.H. 1989. Lacustrine carbonates and pedogenesis: sedimentology and origin of palustrine deposits from the Early Cretaceous Rupelo Formation, W. Cameros Basin, N. Spain. *Sedimentology*, 36, pp 665-684.
- Reineck, H.E., Singh, I.B., 1980. Depositional Sedimentary Environments. Springer, Berlin, pp. 549.
- Sanders, F., Manley, K., Carpenter, K., 2001. Gastroliths from the Lower Cretaceous sauropod *Cedarosaurus weiskopfae*. In: Tanke, D.H., Carpenter, K., (Eds), Mesozoic Vertebrate Life, Bloomington: Indiana University Press, pp.166-180.
- Santos, E.S., Peterson, C.E., 1986. Tectonic setting of the San Juan Basin in the Jurassic. In: Turner-Peterson, C.E., Santos E.S., Fishman, N.S. (Eds.) A Basin Analysis Case Study: the Morrison Formation, Grants Uranium Region, New Mexico. American Association of Petroleum Geologists Studies in Geology # 22, pp 27-33.
- Schudack, M.E., Turner, C.E., Peterson, F., 1998. Biostratigraphy, Paleoecology and biogeography of charophytes and ostracodes from the Upper Jurassic Morrison Formation, Western Interior, USA. *Modern Geology*, 22, pp. 379-414.
- Smith, D.M., 2000. Beetle taphonomy in a recent ephemeral lake, southeastern Arizona. *Palaios*, 15, pp. 152-160.

- Smith, A.E., Hamilton-Taylor, J., Davison, W., Fullwood, N.J., McGrath, M., 2004. The effect of humic substances on barite precipitation – dissolution behaviour in natural and synthetic lake waters. *Chemical Geology*, 207, pp. 81-89.
- Stankiewicz, B.A., 1998. The fate of chitin in Quaternary and Tertiary strata. In: *Nitrogen-containing macromolecules in the bio-and geosphere*, ACS Symposium series, 707, pp. 211-224.
- Suttner, L., 1969. Stratigraphic and petrographic analysis of Upper Jurassic/ Lower Cretaceous Morrison and Kootenai Formations, Southwest Montana. *American Association of Petroleum Geologists Bulletin*, 53, no. 7, p 1391-1410.
- Velde, B., 1995. *Origin and mineralogy of clays*. Springer, New York, pp. 334.
- Weigelt, J., 1989. *Recent vertebrate carcasses and their paleobiological implications*. University of Chicago Press, Chicago, pp. 188.
- Weishampel, D B., Dodson, P., Omlowska, H., (Eds.). 1990, *The Dinosauria*. University of California Press: Berkeley, pp. 733.
- Wings, O., 2004. Identification distribution, and function of gastroliths in dinosaurs and extant birds with emphasis on ostriches (*Struthio Camelus*). Ph.D dissertation, ULB Bonn, http://hss.ulb.uni-bonn.de/diss_online .
- Wright, V.P., Platt, N.H., 1995. Seasonal wetland carbonate sequences and dynamic catenas: a re-appraisal of palustrine limestones. *Sedimentary Geology*, 99, pp. 65-71.

**CHAPTER 3. PALEOENVIRONMENTAL AND PALEOCLIMATIC
IMPLICATIONS OF UPPER JURASSIC MORRISON FORMATION
DEPOSITS, BIGHORN BASIN, WYOMING, U.S.A**

To be submitted as:

Jennings, D.S., Hasiotis, S.T., Paleoenvironmental and Paleoclimatic Implications of Upper Jurassic Morrison Formation Deposits, Bighorn Basin, Wyoming, U.S.A. Journal of Sedimentary Research.

ABSTRACT

Three genetic sedimentary successions in the Upper Jurassic Morrison Formation in the southernmost Bighorn Basin, Wyoming, indicate a change in sedimentation rates and depositional regime between the lower and the upper two successions. In succession 1, sedimentation rates were relatively low between major flooding events and minor channel migration was coeval with associated development of well-drained paleosols. Pedogenic carbonate in the well-drained, composite paleosols indicates that seasonally drier conditions dominated early Morrison time. A change from composite to cumulative paleosols and an abrupt increase in euhedral zeolites and swelling clays signal a change to a more volcanically influenced system with a lower but steadier rate of sedimentation in succession 2. Mottled paleosol horizons suggest seasonally variable drainage conditions. Channel flow remained stable within a relatively restricted channel belt. Palustrine-lacustrine deposition dominated succession 3, producing a mosaic of wetland environments. Fine-grained, smectite-rich material led to sluggish drainage and epiaquatic conditions. Periaquatic edge effects caused lateral

hydrological variability. Increased water alkalinity from altering airfall ash resulted in precipitation of analcime during organic matter accumulation in alkaline marshes and fens. Zeolites, peat deposits, and illite clays indicate a complex palustrine-lacustrine system developed in a relatively closed setting. Overall, sedimentologic, geochemical, and paleopedologic evidence from successions 1-3 suggests that volcanic activity, not climate change, was the driving factor in paleoenvironmental changes in the study area at the end of the Jurassic.

INTRODUCTION

Data collected from the Upper Jurassic Morrison Formation of the Colorado Plateau have resulted in seemingly conflicting paleoenvironmental and paleoclimatic interpretations (e.g. Stokes, 1944; Christiansen et al., 1994; Peterson, 1994; Way et al., 1994; Hasiotis and Demko, 1996; Litwin et al., 1998; Dunagan, 2000; DeCelles, 2004; Dunagan and Turner, 2004; Hasiotis, 2004; Parrish et al., 2004; Rees et al., 2004). Recent research suggests that latitudinal (Demko and Parrish, 1998; Rees et al., 2004) and subenvironmental differences (Parrish et al., 2004) may explain variable data, but the paucity of detailed studies in the northern part of the Morrison depositional basin precludes accurate interpretations. In this study, our objective is to (1) use sedimentary, geochemical, and paleontological data to reconstruct environments of the Morrison Formation in the southeastern Big Horn Basin, Wyoming, (2) assess paleoenvironmental implications of authigenic minerals through the Morrison Formation, and (3) identify the driving factors behind paleoenvironmental changes during the latest Jurassic in the northern Morrison depositional basin.

GEOLOGIC SETTING

During the Late Jurassic-Early Cretaceous, the southern Bighorn Basin area lay midway between a subduction zone to the west and the retreating marine coastline to the northeast (Lawton, 1994). Significant amounts of volcanic debris and ash were transported from the Transcontinental Arc eastward and

northeastward across the Western Interior during Late Jurassic retroarc magmatic events (Suttner, 1969; Peterson, 1972; Santos and Peterson, 1986; Johnson, 1991; DeCelles, 2004). Volcanic activity was more pronounced earlier on the Colorado Plateau (Furher, 1970), progressing northward as the Cordilleran Belt and foreland basin developed together, and the continent moved into a higher latitude (Brenner and Peterson, 1994; DeCelles, 2004). Morrison Formation provenance in the Bighorn Basin changed from a Sevier Thrust Belt source to a distal magmatic source later in the Jurassic (Tabbutt, unpublished data, 1990). Increased sedimentation from plinian eruptions and uplift along the Andean-type magmatic arc increased siliciclastic input. Geochemically unstable volcanic ash altered to smectite-rich sediments in lacustrine environments that developed in the foreland basin (Brenner and Peterson, 1994 pg. 229; Christiansen, et al., 1994). East-northeast flowing rivers transported sediments across the alluvial plain from western highlands as the back bulge migrated to the east (DeCelles, 2004). Subsequent thrust faulting and folding contributed to continued lacustrine development in semi-isolated to isolated basins throughout the Western Interior (Dunagan, 2000).

The study area is located on the Warm Springs Ranch and adjacent BLM lands 1.5 km southeast of Thermopolis, Wyoming, at the southeastern most corner of the Bighorn Basin (Fig. 1). Stratigraphic studies of Morrison Formation outcrops in

the area show deposits representative of a transitional region between the tectonically active zone and more distal parts of the depositional basin subjected to less influential punctuated thrust belt tectonic processes during the Late Jurassic-Early Cretaceous (Douglass unpublished data, 1984). Douglass (unpublished data, 1984) interpreted stacked sandstones west of Thermopolis as avulsion deposits and suggested that the area was a complex fluvial-lacustrine system that resulted from avulsion events during the latest Jurassic.

Erosional unconformities bound the Morrison Formation between the Upper Jurassic Sundance Formation and the chert-pebble conglomerate of the Lower Cretaceous Cloverly Formation (Mirsky, 1962; Furer, 1970).

Throughout ranch outcrops, there is a sharp contact between the glauconitic sandstone of the Sundance Formation and quartz-rich basal sandstone of Morrison Formation. Most of the outcrop area is highly eroded and littered with Cloverly Formation boulders; however, gullies along three east-west trending, south-facing exposures and road cuts near recently excavated dinosaur quarries allow access to relatively open slopes.

METHODS

Stratigraphic Sections

Eight stratigraphic sections were measured and described from freshly exposed trenches using a precision Jacob's staff. Sedimentary descriptions included unit thickness, sedimentary structures, grain size, fossils, and color. Colors were

derived from a Munsell soil-color chart. Vertebrate and trace fossil specimens were left in place after location coordinates, pertinent measurements, and digital photographs were taken. Rock samples were collected from each unit for geochemical analyses and thin sections.

Microscopy

Individual rock samples were analyzed with powder X-ray diffraction (XRD) to identify authigenic mineral compositions. The less than 0.5 μ m size fraction was chosen to limit the detrital clay mineral component. Clays from 72 samples were separated by standard centrifugation methods. Samples were then saturated with 10% KCl and MgCl (Moore and Reynolds, 1997), mounted on glass slides using Drever's Millipore method (1973), and glycolated for two days. Eight samples were heated at 300°C for 1 hour to differentiate clays with 14Å peaks. Mounted clay samples and randomly oriented powdered samples of minerals were analyzed on a SCINTAG XDS 2000 X-ray diffractometer with CuK α radiation at the University of Wyoming, Laramie. Scans were evaluated with methods described in Moore and Reynolds (1997) (See Table 1). Nine representative samples from mudstone facies were analyzed using RockJock and Mudmaster software at the US Geological Survey in Boulder, Colorado. Results were used to provide a quantitative assessment of clay mineral formation processes and for comparative compositional analyses using methods described by Drits et al. (1998) and Eberl (2003).

Sixty-two thin sections of mudstone, carbonate, and nodules from each facies were examined for pedogenic microfabric, microfossils, and other mineralogical characteristics representative of sedimentary environments. Images of representative rock chips from each facies and double-polished thin sections of nodules and carbonates were taken with a Leo 1550 field emission scanning electron microscope (SEM) at the University of Kansas, Lawrence, and a JEOL 5800 LV SEM at the University of Wyoming, Laramie, to compare subtle mineral relationships and morphologies.

Samples of barite associated with dinosaur bones and plant material were analyzed by a continuous flow method on an IsoPrime mass spectrometer at Xymax Stable Isotope Laboratories in California. Values for $\delta^{18}\text{O}$ were reported relative to VSMOW (Vienna Standard Mean Ocean Water) and $\delta^{34}\text{S}$ values were reported relative to V-CDT (troilite of the Canyon Diablo iron meteorite).

STRATIGRAPHY AND SEDIMENTOLOGY

All stratigraphic sections except one in the area measured 50-60 m and are composed of heterolithic sandstone, siltstone, and mudstone units divided into 12 main lithofacies and three genetic successions (Fig. 2). Sections 7 and 8 are located 9 km northeast of sections 1-6. Section 6 measures only 32 m thick where fluvial deposits of the Cloverly Formation cut down and removed the upper half of the Morrison Formation. Sandstone units are limited to sections in the southeastern portion of the study area. Sections 7 and 8 are composed of stacked mudstone units

of varying character. Lithologies above the basal sandstone are laterally variable over short distances and hard to trace for more than 10s of meters. The top 20 m are devoid of sandstone throughout the area. See Table 2 for a summary of facies and facies characteristics.

Sandstone Facies

Description: Off-white and olive gray (5Y6/4) to moderate yellow (5Y6/3) sandstones are predominantly quartzose, calcite-cemented, and fine-grained. Grains are moderately sorted and subangular to subrounded. The majority of the sandstone facies are concentrated in the lower 40 m of all sections.

The basal sandstone is composed of thinly bedded, planar to cross-laminated, tabular sandstones that fine-up and grade into overlying greenish gray shale (5GY2.5/1) or shaly siltstone. Small asymmetrical ripples occur at the tops of the thin sandstone beds. Light olive gray (5Y6/4), trough-crossbedded sandstone units vary in thickness from 2-3 m and are interbedded with off white sandstone units. Dark greenish gray mudstone (5GY4/1) and claystone intraclasts occur in the base of off white sandstone units bounded by thin mudstone packages in the lower parts of sections 3, 4 and 6 (Fig. 2).

Above the lower interbedded mudstone-sandstone units in sections 3, 4, and 6 are stacked, multistory 10-15 m thick, off-white sheet sandstones (Fig. 2). Centimeter-scale, silty sandstone units separate individual sandstones characterized by large trough crossbeds and flat bases in these sections. No coarse channel lag

deposits or lateral accretion surfaces occur at the base of the sheet sandstone units. At the top of multistory sheet sandstones in section 3 is a 2-3 m thick, yellow sandstone bounded with greenish gray, shaly siltstone. A similar yellow sandstone unit occurs approximately 24 m above the basal sandstone in sections 4 and 6. Paleoflow measured from large crossbeds is 12-20° (azimuth) in sheet sandstones throughout the study area.

Three, meter-scale, off white sandstone units located approximately 15 m below the Cloverly Formation contact in unit 1 have a paleoflow direction of 280°. These sandstones have a lenticular geometry, pinch out within 100 m, and contain abundant sauropod bones, silicified and coalified plant material, and sauropod tracks.

Sauropod tracks 40 cm wide in cross section occur in thin, off white sandstone units that are laterally restricted to less than 500 m in section 6 (Fig. 3A-C). Large-scale, trough cross beds can be seen as the sheet thins laterally. Horizontal laminations are prevalent in all sandstone units with abundant tracks. Tracks within this unit have varied morphologies, indicating lateral changes in saturation and length of exposure (Fig. 3A-C). In some tracks, cemented layers within the tracks were pushed down 30-40 cm through bedding. Loading terminates 6-10 cm above the base of the track itself (Fig. 3A, B). Other tracks are less distinct with disrupted sediments infilled with structureless sandstone (Fig. 3C).

Abundant invertebrate traces and small vertebrate tracks and trackways were discovered in slabs weathering down from a 7-m-thick ribbon sandstone in section

6 (Fig. 3D). Tridactyl tracks range in size from 4-20 cm in length and trackways range from three to more than fifteen consecutive tracks. Many of the small tridactyl tracks occur in parallel to subparallel trackways 20-30 cm apart. Morphology of tridactyl tracks varies from distinct outlines with micaceous material in the center to less distinct tracks with phantom outside digits (Fig 3E). Isolated plantigrade tridactyl tracks are found with wedge-shaped impressions near horizontal burrows (Fig. 3F).

Track horizons contain vertical to subvertical smooth-walled tubes and horizontal to subhorizontal, meniscate backfilled burrows with distinct walls. (Fig.3 G). Some vertical tubes occur in pairs. The diameter of the tubes range from 0.5-1.0 cm (Fig.3G).

Along the bedding plane of a sandstone block is a crescent-shaped impression terminating at the end of a trail of disturbed sediment. Two smooth grooves correspond with the middle and one edge of the trail (Fig. 4).

Interpretations: Small scale trough crossbeds, ripple cross laminations, and fining up sequences of the basal sandstone support an interpretation of vertically accreting channel and point bar deposits (Walker and Cant, 1984; Boggs, 1995; Collinson, 1996). Associated light olive gray, trough-crossbedded units interbedded with greenish gray, shaly siltstone are interpreted as levee deposits (Collinson, 1996). Multistory channel sandstones in section 3 are consistent with persistent channel flow in restricted areas (Collinson, 1996). Stream-flow direction for channel deposits was to the northeast throughout the Latest Jurassic.

Laterally restricted sandstone bodies with abundant sauropod tracks are interpreted as crevasse-splay deposits that remained high traffic areas after flooding events. Lenticular, ribbon sandstone units that pinch out to thin sandstone units in section 3 indicate that it was an accretionary bar (Collinson, 1996).

Small- to medium-sized tridactyl tracks are interpreted as theropod tracks and large lobate loading structures are interpreted as juvenile sauropod tracks. Presence of sauropod tracks in crevasse splay deposits suggest that sauropods traveled parallel to a fluvial channel after a major flooding event. Plantigrade tracks with associated wedge-shaped impressions in exposed sandbar deposits are tentatively designated as *Pteraichnus* (Hasiotis, 2004).

Paired vertical burrows interpreted as U-shaped burrows and vertical burrows record shelter burrows of terrestrial and semiterrestrial invertebrates in exposed bar surfaces (Hasiotis, 2002). Crescent-shaped impressions with corresponding trails are designated tentatively as cf. *Koupichnium* (Hasiotis, 2002). These horseshoe crab traces are associated with tropical shallow-water environments with firm substrates (Hasiotis, 2002; Hasiotis, 2004). Burrows are designated tentatively as cf. *Ancorichnus*, cf. *Skolithos*, and cf. *Arenicolites*, respectively (Fig 3F-G). Beetles or soil bugs likely constructed the backfilled burrows in well-drained substrates after soil moisture levels returned to pre-flood conditions (Hasiotis, 2002; Hasiotis, 2004). Tracks, trails, and burrows in the lenticular sandstone show that the bar was often covered with shallow flowing water and supported a diverse fauna.

Siltstone Facies

Description: This facies is composed of two types of siltstone units, a greenish gray siltstone (5Y6/4-5Y6/3), and a black and white laminated siltstone (Fig. 2). Both siltstone types are restricted to sections 3, 4, and 6.

Greenish gray siltstone units are 1-4 m thick, shaly or cross laminated, and loosely cemented with calcite. They are bounded by thin mudstone units associated with trough cross-stratified sandstone or are interbedded with sandstone units.

Black and white laminated siltstones have minor convolute bedding and commonly occur with thinly bedded mudstones and sandstones. Thin sections show laminations are composed of alternating layers of quartz silt and organic matter, similar to rhythmites described by Collinson (1996) and Talbot and Allen (1996).

X-ray diffraction patterns from the siltstone facies show mixed layer smectite-illite clays with subtle variations in percentages of smectite. Samples from the lower part of section 3 have low intensity 001 smectite peaks at 16.9-17 Å and sharper, more pronounced 001 illite peaks at 10 Å, 5 Å, and 3.3 Å. Minor chlorite peaks occur at 7.1 Å, 4.7 Å, and 3.5 Å (Fig. 5 A). Samples from sections 5 and 6 show a well-defined 001 smectite peak that collapses to 14.5 Å with KCl saturation (Fig. 5 A). Peak intensity of the 001 14.5 Å peaks increase in heated samples and the 002 peak occurs just above $25^\circ 2\theta$, suggesting they are 001 chlorite peaks rather than vermiculite (Moore and Reynolds, 1997). Although some samples

contain a small percentage smectite layers, illite is the primary clay contained in siltstone facies.

Interpretation: Both siltstone types are interpreted to have been deposited in low-lying areas immediately adjacent to a main fluvial channel. Greenish gray siltstones were deposited near the channel on levees and in adjacent, poorly drained proximal floodplain areas (Walker and Cant, 1984; Collinson, 1996). Well-laminated siltstones that have rhythmic laminations are also associated with floodplain or abandoned channel deposits (Collinson, 1996).

Red Mudstone Facies

Description: Dark reddish brown to reddish brown (2.5YR3/3 5YR4/3) mudstone units composed of silty clay are generally massive and 50-100 cm thick (Fig. 2). No primary sedimentary structures are present. Well-preserved, micrometer-scale rhizoliths with filamentous hairs are preserved in some samples (Fig 6 A). Thin sections show angular-subangular, silt-sized quartz grains cemented by iron oxides (Fig. 6 B). Calcite-coated grains float in a clay-rich matrix with scattered fragments of ooids and abraded shell fragments (Fig. 6 B, C). Calcite nodules and rhizoliths with remnant organic material are common (Fig. 6 D). Minor stubby zircon crystals with alteration haloes occur in samples from lower units. Units with stubby zircon crystals commonly overlie centimeter-scale, nodular, micritic calcite units and greenish gray mudstone.

Red mudstones occur in stacked successions with olive or greenish gray mudstone and few carbonate units in sections 7 and 8 (Fig. 2). Greenish gray mudstones have sporadic black or red mottling. Mottles are irregular to elongate in shape. Boundaries between the matrix and the mottles are diffuse. Olive gray mudstone (5Y5/2) underlying red mudstone units have irregular to elongate brown or lighter olive gray mottles (5Y6/3-5Y6/2). Red mudstone units in section 8 have green mottles.

In section 7, three spherical structures 32 cm in diameter, spaced about 3 m apart and composed of red mudstone, are found in a 30-40 cm light greenish gray mudstone unit (Fig. 6 E). A few mottles occur along the edge of one side toward the base of the structures. The red mudstone in the structure is compositionally similar to the overlying red mudstone, although it is a little lighter in color with whitish edges. No organic matter is associated with the structures.

Clay composition changes little in red, olive gray, and greenish gray horizons. Illite with minor chlorite in these samples is recognized by clear 10 Å, 5 Å, and 3.3 Å peaks (See fig. 5 B). Peak intensity increases slightly with KCl saturation, but peak position and peak width remains the same for samples from all sections.

Interpretations: Red mudstone units are interpreted as the topmost mineral horizons (A) of relatively well-drained, moderately developed, floodplain and levee paleosols that developed on reworked glauconitic deposits from the Sundance Formation. See Fig. 6 F for representative profile. Nodular, micritic calcite units accumulated as pedogenic carbonate (Bk) horizons in well-drained soils as a result

of translocation of Ca-rich material down through the soil during the rainy season and precipitated at the depth of seasonal wetting during dry seasons (Wright and Tucker, 1991; Retallack, 1997). Rhizoliths in these paleosols indicate that the landscape was vegetated.

Associated olive gray and greenish gray mudstones are similar to reduced subsurface paleosol (Bg) horizons described by Retallack (1997) and Kraus (1999) and indicate that the area was inundated during the wet season. Gleyed B horizons remained saturated due to a shallow groundwater table in areas proximal to the channel and low-lying areas distal from the channel (e.g. Vepraskas, 2001). Mottles are interpreted as redoximorphic features, indicating fluctuations in local hydrology (Kraus, 1997; Kraus and Guinn, 1997). Black mottles resulted from translocation of Mn when the soil was saturated during the wet season and reprecipitated along pore linings when the soil was better drained (Davies-Vollum and Kraus, 2001; Vepraskas, 2001). Redoximorphic features in sections 7 and 8 resulted from associated short-term fluctuations in hydrology in lower areas distal from the channel during the wet season. High water tables resulted in gleyed horizons lower in the profile (Kraus, 1999). Upper horizons remained relatively drier after infiltration of surface water (Kraus, 1999). Decreased sedimentation rates between intermittent flooding events resulted in composite paleosol development on floodplain sediments between infrequent flooding events (Kraus, 1997).

Spherical, red mudstone structures in light greenish gray horizons distal from the channel are interpreted as large-diameter burrows. Overlying gleyed clay-rich mudstone suggests that the cavity was infilled after the lower horizon was gleyed. Similar large diameter burrows, interpreted as fossorial mammal burrows, have been reported from the Upper Triassic Chinle Formation and Upper Jurassic Morrison Formation (Hasiotis, 2002, 2004; Hasiotis et al., 2004). Recently a body fossil of a fossorial mammal was reported from Upper Jurassic deposits in Colorado (Luo and Wible, 2005). Burrows similar in shape are primarily used for shelter from heat during the dry season by modern monotremes and multituberculates in distal floodplains (Platt et al., 2004).

Although illite and chlorite are common clay minerals found in hot-dry climates (Chamley, 1989), reworked glauconitic sands and silts likely provided the parent material for these paleosols and subsequent illite-chlorite clay composition. Ryan and Hillier (2002) documented chlorite in Wyoming Sundance Formation deposits, suggesting that the chlorite component is likely a remnant of the parent material.

Olive Mudstone Facies

Description: Olive to olive gray (5Y5/3-5Y5/2) mudstone units occur in association with red mudstone and greenish gray mudstone in all sections except section 5 (Fig. 2). Units vary in thickness from 0.3-1.0 m in lower Morrison deposits to 2.0-5.0 m thick in section 7. These mudstones contain a little more silt than other mudstones,

particularly at contacts with greenish gray units. Plant fragments, light olive mottles, and small iron and manganese nodules are common. Long, euhedral zircon crystals with no alteration haloes are abundant in section 7 just above the red paleosols. Microcline and a few augite crystals occur with calcite-coated quartz grains suspended in a clay matrix. Occasional thin siltstone and fine-grained sandstone lenses occur in the stacked olive gray mudstone units in section 7. XRD patterns of olive gray mudstone show illite-smectite mixed layer clays with minor chlorite (Fig. 7 A). Smectite peaks do not fully collapse with KCl saturation and do not show a clear chlorite peak at 14.5 Å, indicating the presence of vermiculite layers in the crystal lattice. Units with increased zircon abundance show feldspar peaks at 3.2 Å and calcium peaks at 3.04 Å.

Interpretation: Based on leaching and translocation of clays and iron in reduced horizons indicated by vertical increasing abundance of mottles, stacked, olive gray mudstone units are interpreted as composite, poorly drained paleosols. Composite paleosols in sections 7 and 8 likely resulted from a steadier rate of sedimentation coincident with an increase in zircon abundance (Kraus, 1999). Zircons, microcline, and augite signal an abrupt increase in volcanic influence during the late Morrison time. Lighter olive gray mottles suggest extended periods of saturated soil conditions that resulted in leaching of iron along root pores and soil-pore linings (Vepraskas, 2001).

Greenish Gray Mudstone Facies

Description: Dark greenish gray to light greenish gray (10GY5/1 and 10GY6/1) mudstone units are found both in association with purple mudstone facies or interbedded with well-indurated, light gray (N7) carbonate mudstone in the uppermost part of all sections (Fig. 2). Units commonly contain 20% silt but are much more clay-rich when associated with purple mottles. Mudstone varies from 0.5-1.0 m thick to 1.0-5.0 m thick. Units interbedded with carbonate mudstone have desiccation cracks 10-20 cm deep, slickensides, and sparry calcite infilling cracks.

Interbedded carbonate mudstone-greenish gray mudstone successions are located 12-15 m from the contact with the Cloverly Formation in sections 1-5. Carbonate mudstone and associated black claystone yield conchostracans and ostracodes. Well-preserved dinosaur fossils are abundant in the carbonate mudstone. Sparse, poorly preserved bone fragments occur in the greenish gray mudstone. Carbonate nodules in greenish gray mudstone occur either as masses with indistinct boundaries with the matrix or as oval to rounded nodular masses with sharp contacts with the surrounding matrix. Invertebrate burrows and rhizoliths are abundant in some units. In one dinosaur quarry, barite nodules are closely associated with bones. Greenish gray mudstone is compacted preferentially around them, indicating barite precipitated prior to significant burial.

Three meters below the Cloverly Formation contact in section 1, a 1 m thick nodular, weathered carbonate mudstone underlies a purple-mottled, greenish gray

unit. Thin sections show micritic calcite and chalcedony infilling pores and brecciated bone fragments. Illuviated clay and sparry calcite infills cracks between limestone nodules and centimeter-scale fissures.

Interpretations: Greenish gray mudstone units are interpreted as gleyed, hydric paleosol horizons that accumulated in palustrine-lacustrine environments where the water table was at or near the surface most of the time. Chroma less than 1 or 2 indicates a consistently high water table and reducing conditions (Vepraskas and Faulkner, 2001). Assuming that the parent material was not greenish gray, mottle-free, greenish gray units represent poorly drained areas that restricted the movement of iron in reducing conditions and were seldom dry enough to be oxidized (Vepraskas, 2001).

Conchostracans and ostracodes in interbedded carbonate mudstone-greenish gray mudstone units suggest these units accumulated in transitional palustrine-lacustrine zones near shallow, ephemeral water bodies similar to those described by Platt (1989). Fluctuating subaqueous and subaerial exposure resulted in alternating accumulation of carbonate mud and poorly developed reduced paleosols.

Barite nodules form where sulfate-rich and barium-rich fluids converge (Hanor, 2000) either by hydrothermal water entering sulfate-bearing marine waters or as a result of microbially induced early diagenetic precipitation within 1 m of the sediment-water interface (Br  h  ret and Brumsack, 2000; Hanor, 2000). Since there is no indication that the Morrison deposits in the study area were metamorphosed or hydrothermally altered, conditions for localized barite

precipitation were facilitated by oxidation of thiols released by putrefaction of organic material.

The brecciated-nodular structure of the carbonate mudstone underlying the purple-mottled, greenish gray unit suggests it was a palustrine carbonate mudstone pedogenically modified as plants invaded the exposed surface during a prolonged dry phase (Armenteros, 1998). The decay of organic material and alteration of smectite clays under reducing conditions allowed chalcedony and calcite to infill soil pores (Alonso-Zarza, 2003). Continued seasonal wetting and drying produced microkarst that later filled with sparry calcite.

Greenish Black Siliceous Claystone

Description: A greenish black (5GY2/1), indurated unit crops out 22 m below the Cloverly contact in sections 7 and 8 (Fig. 2). This highly resistant unit can be traced for a kilometer or more along the outcrop. Remnant desiccation cracks are apparent on the top of the bed and no bedding is noticeable. Thin sections show radial quartz crystals with liquid fluid inclusions and organic material in a fine-grained, green matrix (Fig. 8A). Angular quartz and muscovite mica also occur in the green matrix (Fig. 8B). XRD scans indicate there is natrolite present with chlorite and quartz in a carbonaceous matrix.

Interpretation: All-liquid fluid inclusions in quartz support a low temperature, shallow burial environment of precipitation. As fine-grained, rhyolitic or dacitic ash altered in aqueous environments, zeolites and quartz precipitated out of

porewater similar to deposits in modern systems in Africa (Ashley and Driese, 2000). The presence of carbonaceous material suggests abundant vegetation in the vicinity during the deposition of this unit.

Purple Mudstone Facies

Description: Grayish purple to grayish red purple (5P4/2; 5P6/2; 5RP4/2) mudstone facies are 1-6 m thick and are dominantly composed of clay with some silt.

Slickensides occur in the top of some units (Fig. 2). Green, red, and gray mottles are abundant. Large conical, carbonate steinkerns with barite cores co-occur with micritic carbonate-coated, lignitized tree trunks and large nodular barite concretions in section 2 (Fig. 8C). Iron-oxide concentrations surround carbonaceous material (Fig. 8D) and line arcuate fractures in this interval with unidentifiable, poorly preserved dinosaur bone. Dinosaur bone fragments contain dissolution features and lack cortical bone (surface bone).

Clay compositions in purple mudstone are predominantly mixed layer smectite-illite and increase in percent illite in associated dark greenish gray mudstone intervals (See Fig. 7B). Quartz and feldspar peaks occur in XRD scans of clay-rich units even though little silt or feldspar is observed in thin section.

Interpretation: Purple mudstones are interpreted as cumulative hydromorphic paleosols that were subjected to extended saturated conditions and steady sedimentation rates (Kraus, 1999). See Fig. 8 F for a representative profile. Redoximorphic features indicate variable hydrology during wet seasons in an

otherwise well-drained and forested paleosol (Kraus, 1997; Hurt and Carlisle, 2001; Vepraskas, 2001). Subsequent drier conditions caused oxidation of translocated iron concentrations around roots and pore linings in the soil (Kraus, 1999; Vespraskas, 2001). Greenish gray clay-rich mudstone units underlying purple mottled mudstone are interpreted as lower subsurface horizons with translocated clay accumulation (Btg). Fluctuations in the water table produced slickensides in upper Bg horizons and caused translocation of clays to reduced horizons in distal floodplain areas during the latest Jurassic (Kraus, 1999).

Extensive flooding resulted in drowning of a waterlogged forested area in the western part of the field area. Decaying organic matter created conditions favorable for early diagenetic barite precipitation. Highly reducing conditions that caused Fe²⁺ mobilization contributed to degradation of bones buried in these units (Behrensmeyer et al., 1989).

Black Mudstone Facies

Description: Black (N2), clay-rich mudstone facies are 1.0-2.0-m-thick units that have no primary sedimentary structures (See Fig. 2). Fragments of plant material are abundant in sediments. Fragmented and whole ostracode shells are found in an upper unit of section 3. Four articulated and complete, adult *Camarasaurus* skeletons were removed from this unit and the underlying carbonate mudstone. Two compressed lignitized tree trunks with well-preserved bark texture lay on top of one skeleton. Rib bones show spiral or helical splitting around the

circumference of the shaft along the grain. Calcite mineralization is evident along fractures. XRD patterns indicate primarily illite clay composition for these units (Fig. 9A).

Interpretation: Black mudstone facies are interpreted as marginal wetlands associated with palustrine-lacustrine deposits in sections 1 and 2. The presence of both bone and abundant plant material suggests fluctuating redox conditions. Groundwater movement can cause mineralization of bone, producing the same kind of CaCO₃ mineralization in fractures as seen in specimens from section 3 (Irving et al., 1989). Spiral splitting of cortical bone material is indicative of brief subaerial exposure before burial (Behrensmeyer et al., 1989). Organic-rich deposits accumulate in areas that have abundant vegetation and low-lying areas that have sluggish drainage, primarily depressional or sloping wetlands (Collins and Kuehl, 2001). The groundwater table was likely at or above the surface in localized low-lying areas for most of the year.

Greenish Gray Claystone Facies

Description: Dark greenish gray to greenish gray (10Y5/1 to 5GY5/1) claystone units are 4.0-5.0 m thick and are composed of clay with little or no silt (Fig. 2). No primary sedimentary structures or pedogenic features are evident, however, intervals that underlie black claystone have 20-30 cm of apparent oxidized material at the top. Sediments appear to be devoid of macrofossils except for an accumulation of organic-rich nodules in section 4. The mound of nodules is 1.5 m

x 0.4 m in outcrop vertical section. Oval-shaped nodules range in size from 5-9 cm in diameter and are vertically compressed. Illuviated clay infills space between the nodules. Thin sections show well-preserved woody plant tissue and amorphous masses in a fine-grained matrix (See Fig. 8E). No other plant material is apparent in these units.

XRD scans indicate a clay composition of illite with minor chlorite. Peaks at 10Å, 5 Å, and 3.3 Å get sharper when saturated with KCl. Chlorite peaks are very minor (Fig. 9B).

Interpretation: Greenish gray claystone facies are interpreted as reduced wetland environments where deeper, slow moving water stood above the surface for much of the time. The absence of mottling and pedogenic features suggest that these horizons were never subaerially exposed (Pipujol and Buurman, 1994; Vepraskas, 2001). Samples of horizons begin to oxidize with exposure to air, indicating that there was no translocation of Fe^{2+} through permanently waterlogged sediments (Vepraskas, 2001). The paucity of plant material and silt- and sand-sized sediments implies that these environments received little or no overland flow from streams and may infer a thickened mineral accumulation under a long-lived, mineral wetland soil (Richardson et al., 2001).

Black Claystone Facies

Description: Black (N1) claystone is subdivided into two subfacies, a massive organic-rich claystone and a laminated unit with abundant wood and plant

fragments. The black claystone units vary from 1.0-7.0 m thick and immediately overlie greenish gray claystone units in sections 1, 5, and 7. Thin sections show rounded, low relief masses with a darker colored rind on the outside with microscopic organic matter in a clay-rich matrix (Fig. 10 A). Sulfur leaches out from both types of black claystone subfacies. XRD patterns show illite peaks at 10Å, 5 Å, and 3.3 Å and minor 7.1 Å, 4.7 Å, and 3.5 Å peaks in both MgCl and KCl saturation. Quartz peaks occur at 4.2 Å and 3.3 Å. Powder XRD patterns of laminated claystone indicate a composition of abundant analcime, quartz, and carbonaceous material (Fig. 9 B).

In sections 7 and 8, the black claystone is overlain by 8.75 m of laminated, organic-rich claystone. This unit extends for more than 2 km along the outcrop, thickening to the east. Analcime crystals are well distributed throughout the deposits (Fig. 10 B). Compressed fern pinnae, seeds, lignitic woody fragments, and leaf fossils are abundant in the deposit.

Interpretation: Black claystone facies are interpreted as hydric soil horizons similar to those horizons documented in open wetland and associated analcime-rich peat deposits in Africa (Ashley and Driese, 2000) and Minnesota (Collins and Keuhl, 2001). See Fig. 10 C for representative profile. Degraded organic soil material accumulated in lower sapric Oa horizons of wetland soils by the decomposition of organic matter and subsequent buildup of organomineral complexes. Microscopic rounded masses are interpreted to be fecal pellets of detrital feeding invertebrates and insect larvae (Craft, 2001). In modern hydric soils, similar residual aggregates

of organic material, also called organic bodies, have been documented in Oa horizons (Vepraskas, 2001).

Shallow, very poorly drained settings adjacent to vegetated wetland areas in the upper part of sections 7 and 8 allowed extensive peat deposits to accumulate in overlying fibric Oi horizons (e.g., Collins and Keuhl, 2001). Decayed organic matter accumulated in a waterlogged, stagnant fen overlying clay-rich wetland mineral soil horizons. Mineralization of dissolved organic carbon (DOC) resulted as DOC adsorbed onto clays contributed by overland flow during infrequent flooding events and from alteration of fine-grained volcanic ash (Collins and Keuhl, 2001). Alkaline conditions indicated by increased illite clays and abundant early authigenic analcime suggest that evapotranspiration was a dominant process in this wetland environment. Similar conditions existed for Quaternary lacustrine deposits in low latitude semiarid regions (Hay, 1970; Surdam and Eugster, 1976; Renaut, 1993).

STRATIGRAPHIC AND GEOGRAPHIC DISTRIBUTION OF AUTHIGENIC MINERALS

Clays, barite nodules, analcime, and quartz are the main authigenic minerals in the study area. Geographic and stratigraphic distribution of authigenic minerals are facies specific (See Table 1). Iron is abundant throughout the deposits and inherent in most clay minerals. With the exception of clays in the red mudstone, all authigenic minerals formed in the top two successions of the Morrison (see Fig. 2).

Clays

Authigenic clay formation is related to both parent material and paleoenvironment based on analyses of clay minerals (See figures 5, 7, and 9). Red paleosols contain primarily illite with minor amounts of chlorite. Lower olive gray and greenish gray horizons of red paleosols also contain minor components of smectite and chlorite in addition to high percentages of illite. Illite was likely a weathering product as well-drained paleosols developed on glauconitic sediments in the lower part of the Morrison Formation (Meunier and Velde, 2004). Chlorite inherent in the parent material remained a small component in lower horizons. Well-drained paleosols in the upper units developed on more volcanically influenced alluvial deposits and are composed of a high percentage of illite with minor vermiculite and chlorite as a weathering product of feldspars in more alkaline environments (Meunier and Velde, 2004).

Olive gray mudstones not associated with red paleosols are rich in smectite-illite mixed-layer clays with minor chlorite. Rhyolitic-dacitic volcanic ash altered in saturated conditions results in degradation of early smectite clay to smectite-illite mixed layer clays (Chamley, 1989; Hillier, 1995). Purple mudstone facies are also rich in smectite-illite mixed-layer clays. It is important to note that the smectite content of clays increases near paleosol units with abundant zircons and plagioclase, suggesting input of larger quantities of ash material and less reducing conditions at those intervals. Volcanic material at this level is assumed to have

been less weathered because saturation by surface water was limited due to either an extended dry period or shorter wet seasons.

Vermiculite-illite mixed-layer clays occur in the greenish gray mudstone interbedded with carbonate mudstone. Clays in carbonate mudstone units are Ca-Mg smectite, a common clay mineral associated with alkaline lacustrine environments (Chamley, 1989; Hillier, 1995). Smectite-vermiculite-illite mixed-layer clays occur where greenish gray mudstone intervals are not associated with carbonate mudstone. Vermiculite-illite is a common mixed-layer clay found in volcanic soils (Chamley, 1989). Predictable patterns of smectite-rich deposits alternating with vermiculite-illite mixed layer clays in palustrine-lacustrine deposits are reasonable in a fluctuating alkaline aqueous system that receives airfall ash (Hillier, 1995; Moore and Reynolds, 1997).

Black mudstone and greenish gray claystone scans indicate the presence of illite. Illite is found in modern wetland and lacustrine systems that are volcanically influenced (Chamley, 1989; Moore and Reynolds, 1997). Organic acids and bacterial activity partly degrade or destroy smectite, in strongly reducing conditions, (Chamley, 1989). Consequently, it is reasonable to expect illite to be a clay associated with underclays in the volcanically influenced wetland soils in the upper part of the Morrison Formation.

Barite

Barite nodules occur in only two units; a purple-mottled mudstone approximately 6 m below the Cloverly Formation contact and packed around dinosaur bones in a quarry 12 m below the Cloverly Formation contact in section 1. As a rule, equilibrium prevails in barite formation at only low pH and high temperatures. Kinetic factors govern precipitation at low temperatures even with low pH (Hanor, 2000). Consequently, kinetic processes dominate barite formation in most environments. Because kinetic processes in barite isotopic exchange are very slow, oxygen and sulfur compositions record the sources and processes that initially produced sulfate (Seal et al. 2000). Oxygen isotope composition varies between 6-10‰ VSMOW, suggesting a freshwater signature for the fluid of formation. Sulfur isotopes have values between 10-14‰ CDT, supporting the interpretation that the source of sulfate was oxidized thiols from the decaying organic matter. Increased barium concentrations in volcanically influenced wetland soils similar to those described by Ashley and Driese (2000) would have provided an ample source of barium for barite precipitation within the microenvironment created by the decaying organic material in shallow water settings.

An alternative source of barium is a concentration in the bone and plant material resulting from incidental ingestion of barium-rich sediments or barium storage in plant tissue. Barium, as with other alkaline earth elements, tends to be stored in spongy bone tissue rather than expelled from the body (Atun and Bascetin,

2003). This explanation makes it difficult to explain the preferential precipitation of barite around bone material, particularly against well-preserved cortical bone.

Analcime and Quartz

Analcime is well documented in organic-rich deposits as a product of altering volcanic ash in aqueous environments (Hay, 1970; Taylor and Surdam, 1981; Renaut, 1993). Highly reactive airfall ash deposited in water quickly alters to smectite clay and siliceous gel. As alkalinity increases during the alteration process, zeolites form in areas of concentrated ions (Drits et al., 1997; Calvo et al., 1999; Meunier and Velde, 2004). The abundance of euhedral zircons, smectite, and authigenic quartz in the upper 2 successions suggests that Morrison Formation deposits continued to be volcanically influenced during latest Jurassic (see Fig. 10B).

Analcime formation reported from Quaternary nonvolcaniclastic sediments are usually associated with kaolinite (Surdam and Eugster, 1976; English, 2001) and in fissures, veinlets, and geodes associated with hydrothermal genesis (Gottardi and Galli, 1985; Utada, 1988). No kaolinite or indications of hydrothermal deposits are documented in local Morrison deposits. Radial quartz crystals with matrix inclusions suggest that silica precipitated out of solution as silica-rich ash altered in water. It is reasonable to interpret the co-occurrence of early diagenetic zeolites, carbonaceous material, and radial quartz crystals as altered volcanic ash deposited in an aqueous environment.

DISCUSSION

Three genetic successions in the study area correspond to changes in hydrology and sedimentation rate (see Fig. 2). Stratigraphic sections described by Douglass (unpublished data, 1984) 5 km west of Thermopolis, Wyoming, show similar successions and parallel changes in lithologies. The absence of sandstone units above the basal sandstone in sections 7 and 8 indicate that this part of the study area was distal to a fluvial channel throughout most of Morrison time. The limited occurrence of multistory sheet sandstone units in sections 1-6 indicate that channel migration was restricted to a rather narrow channel belt in the west, flowing to the northeast. The overall geometry of the area remained constant through Morrison deposition. Figures 11 A-C show the depositional system changes for each succession.

Succession 1 consists of interbedded mudstone and sheet sandstone in western sections (Fig. 11 A). Correlative composite, red paleosols with pedogenic carbonate suggest these soils formed during seasonal wetting and drying. Mottled, greenish gray- and olive gray-lower horizons indicate changes in redox conditions due to seasonal fluctuations in saturation (Kraus, 2002). Gleyed, greenish gray horizons were subjected to prolonged groundwater saturation and indicate a shallow water table. Moderately developed, composite paleosols suggest a comparatively moderate rate of accumulation between flooding events that reached the distal floodplain. Poorly developed, well-drained levee paleosols and siltstone suggest

that channel migration occurring during this time was restricted to a relatively narrow channel belt.

Succession 2 shows an abrupt decrease in sedimentation rate and a change in drainage conditions associated with a concurrent change in clay mineralogy and zircon abundance (Fig. 11 B). Zircon morphology associated within these intervals suggest an increased input of rhyolitic and dacitic ash material. Mottled purple and greenish gray horizons indicate saturated conditions were longer lived during deposition of this succession (Kraus, 2002). An increase in swelling clay composition hindered drainage conditions. Gypsum found in floodplain deposits west of Thermopolis (Douglass unpublished data, 1984) suggests a continued low precipitation to evaporation ratio.

Burrows and rhizoliths in paleosols near channel deposits and abundant mottles in paleosols distal from the channel imply the presence of organisms tolerant of frequent flooding or intermittent standing water and variable redox conditions (Hasiotis, 2000). Abundant dinosaur tracks and invertebrate trace fossils in point bar deposits indicate the area supported a diverse fauna that included horseshoe crabs, pterosaurs, small theropod dinosaurs, and abundant semi-terrestrial and terrestrial invertebrates. Sauropod tracks and body fossils found in crevasse-splay deposits and associated with large theropod tracks in lacustrine carbonate mudstone suggest larger animals frequented lacustrine environments.

Fluvial deposits are more restricted throughout succession 3 and end with 3 successive crevasse-splay deposits 15 m below the Cloverly Formation contact in

section 1-3. The top 12 m of Morrison deposits are devoid of sandstone throughout the study area. Cumulative hydric and hydromorphic paleosols with little preservation of carbonaceous shales suggest that sedimentation rate was slow enough to allow continuous pedogenic development over an extensive time (Davies-Vollum and Kraus, 2001).

Variations in facies in succession 3 show subtle topographic differences within an extensive, low gradient wetland-lacustrine system (Ashley and Driese, 2000; Hurt and Carlisle, 2001) (See Fig. 11 C). Organic-rich deposits and gleyed claystone suggest that the water table was at or above the surface for long periods (Hurt and Carlisle, 2001). Adjacent mottled paleosols and interbedded lacustrine carbonate mudstone and gleyed mudstone developed in fringe areas more susceptible to large-scale fluctuations in hydrology. Palustrine and pedogenic carbonates commonly form in semiarid climates and may indicate reduced clastic input and aggradation of a floodplain (Alonso-Zarzo, 2003).

Purple mudstone and mottles occur in areas that were topographically higher on the landscape but still subjected to substantial periods of saturation. Long periods of saturation and consequent mobilization of Fe^{2+} alternated with better-drained conditions, resulting in Fe_2O_3 concentrations along root pores and fracture planes within paleosols (Davies-Vollum and Kraus, 2001). Thick mucky units delineate areas of open water that were likely protected from clastic input where organomineral material accumulated (e.g., Hurt and Carlisle, 2001).

An increase in plant material in reduced units in sections 5, 7, and 8 suggests that the area was persistently saturated and relatively anoxic in some areas.

Vegetation, particularly woody plants, was abundant enough to support a diverse population of sauropods. Peat accumulated in thick deposits in surrounding fens (e.g., Collins and Kuehl, 2001). Cycad steinkerns with barite cores and calcite coated tree trunks suggest that a wooded area was inundated and drowned with water. Overlying reduced mudstone and mucky claystone indicate the fringe area was permanently flooded for the rest of Morrison time.

Authigenic minerals throughout succession 3 suggest that the system was highly alkaline with fluctuations in oxic and anoxic conditions. Ca-Mg smectite units interbedded with vermiculite-illite mixed-layer clays accumulated at the fringe of the wetland-lacustrine areas while illite-rich hydric paleosols developed in more reduced, saturated fens and marshes. Low temperature analcime precipitation within similar environments suggests that a semiarid tropical climate prevailed (Hay, 1970; Ashley and Driese, 2000; English, 2001). Coincident precipitation of quartz indicates that volcanic material altered in an aqueous subenvironment within a relatively closed wetland-lacustrine system.

CONCLUSIONS

Mudstone bounded sandstone units and multistory channel sand bodies in succession 1 document a moderately high rate of short-lived migration events within a narrow channel belt (Makaske, 2001; Slingerland and Smith, 2004) during

the earliest Late Jurassic time. Crevasse-splay deposits, and thin ribbon and sheets sand combined with composite, well-drained paleosols with pedogenic carbonate indicate that a strongly seasonal climate is the dominant signature in this depositional sequence. Pedogenic and palustrine carbonates suggest a semi-arid climate dominated throughout Morrison deposition (Alonzo-Zarza, 2003).

The abrupt transition from well-drained environments in succession 1 to a more volcanically influenced, increasingly less well-drained environments in successions 2 and 3 presents a more difficult challenge when interpreting possible allogenic factors. Sedimentary response to volcanic events have not been considered in previous interpretations of strata in the Morrison Formation even though major episodes of volcanism have been documented (DeCelles, 2004).

Modern studies indicate that sedimentation increases exponentially within a volcanically influenced fluvial system (Smith, 1988; Major et al., 2000; Gran and Montgomery, 2005; Kataoka, 2005). Recovery of the fluvial system can be a long-lived process hampered by recurring volcanic events (Gran and Montgomery, 2005). Easily erodible and highly reactive sediments are directed through an immediately overburdened fluvial system. Avulsion rates increase as much as ten fold as tributaries and main channels are inundated with sediments (Gran and Montgomery, 2005). Tributary streambeds near the source aggrade as much as 4 m/year and flow is completely restricted within 3-4 years, resulting in flooded drainage areas (Kuenzi et al., 1979; Gran and Montgomery, 2005). Fluvial and ecological recovery progresses from proximal to distal areas (Gran and

Montgomery, 2005). It is likely that fluvial system recovery after major plinian eruptions in the latest Jurassic was similar to modern systems.

Although few studies have documented fluvial recovery in areas more than 50 km from a volcanic source, it is reasonable to expect that extensive alkaline palustrine-lacustrine systems may develop on the distal alluvial plain without a significant climatic change because of increased influx of fine-grained, altered ash (Kuenzi et al., 1979). Consequently, assessment of Morrison Formation deposits requires integration of sedimentary, geochemical, and paleontological data to evaluate climatic and environmental responses to volcanic events.

Authigenic mineral assemblages in the Morrison Formation, including clay mineral compositions, are similar to those documented in African wetland-lacustrine systems (Hay, 1970). Lateral patterns of clay distribution in palustrine-lacustrine deposits at the top of succession 3 are consistent with those documented in alkaline lakes and wetlands in tropical, semiarid climates (Hay, 1970). An increase in precipitation would more likely result in acidic soil conditions and increased weathering of clay minerals (Righi and Meunier, 1995; Collins and Kuehl, 2001).

Soils in volcanically influenced environments may contain clays that correspond to predictable climate related weathering (Chamley, 1989). In temperate climates, smectites dominate, however, warmer and wetter conditions result in higher percentages of kaolinite, degrading to oxide clays in persistently wet tropical environments (Chamley, 1989; Righi and Meunier, 2001). It is

important to note that discrete clay mineral assemblages within the same depositional and climatic regime in alkaline-saline, wetland-lacustrine systems (Hay, 1970) correspond to parent material rather than climate.

Few data have been compiled on authigenic minerals in systems receiving rhyolitic-dacitic volcanic material with different climates. Consequently, the assumption that modern systems in Africa are analogous enough for reasonable comparisons of authigenic mineral assemblages remains less than definitive. Soils in South America (Beek and Brama, 1968) and Central America that have received reworked rhyolitic-dacitic ash from the magmatic arc may provide better comparisons with Morrison paleosol distributions and geochemical signatures. Widespread shallow-water palustrine-lacustrine systems that developed quickly in response to Guatemalan volcanic events (Kuenzi et al., 1979) may also offer valuable insight into geochemical, sedimentary, and ecological recovery in similar climates in ancient settings.

Clay mineral composition in the Morrison Formation can vary widely depending on the subenvironmental facies within an individual stratigraphic section. Subenvironments within a volcanically influenced system vary significantly within short distances. As a result, general vertical trends averaging clay composition over 100s of meters of clay-rich deposits may be misleading. The clay change proposed by Turner and Peterson (1999) is not observed in the study area. Instead, clay compositions are more closely associated with environmental conditions and parent material. Abundant illite in succession 3 makes it impossible

to use clay composition as a tool to place fossils in any stratigraphic context or correlate strata. Clay composition is not a valuable correlation tool for any deposits in an area separated by more than a kilometer. Trujillo (unpublished data, 2003) documented similar trends in other Morrison Formation deposits in Wyoming.

The decreased diversity near the end of the Morrison Formation proposed by Turner and Peterson (1999) are not supported in central Wyoming. Trace- and body fossil data suggest that a diverse population of vertebrates and invertebrates including pterosaurs, theropods, sauropods, horseshoe crabs, insects, and plants populated the area during the Late Jurassic. The increase in volcanic input did not appear to affect the biodiversity; however, increased alkalinity may have increased the preservation potential of many fossils through earlier cementation and permineralization due to higher pH and carbonate saturation (Martin, 1999).

Apparent contradictory sedimentary and paleontological data have resulted in conflicting Late Jurassic paleoenvironmental interpretations. Paleobotanical data suggest that the climate during the latest Jurassic was humid and wet (Tidwell, 1990; Ash, 1994) while sedimentary data and climatic models suggest a drier, more temperate climate (Demko and Parrish, 1998). Parrish et al. (2004) suggest a change to a humid, semiarid climate from the Kimmeridgian to the Tithonian, and Hasiotis (2004) interprets a more tropical wet-dry climate. Results of this study suggest that geochemical changes in the Morrison depositional basin in the southern Bighorn Basin masked any climatic signature. Zeolites, clay mineralogy, gypsum precipitation, and pedogenic carbonates suggest a persistent tropical semiarid

climate. Avulsion deposits are not widespread in the area and major flooding events were likely related to fluvial recovery processes after massive plinian eruptions. Combined geochemical and sedimentary data support that volcanic activity not climate was the primary factor governing paleoenvironmental change at the end of the late Jurassic in Wyoming.

REFERENCES

- Alonzo-Zarza, A.M., 2003, Palaeoenvironmental significance of palustrine carbonates and calcretes in the geological record: *Earth Science Reviews*, v. 60, p. 261-298.
- Ash, S.R., 1994, First occurrence of *Czekanowskia* (Gymnospermae, Czekanowskiales) in the United States: *Review of Palaeobotany and Palynology*, v. 81, P. 129-140.
- Ashley, G.M. and Driese, S.G., 2000, Paleopedology and paleohydrology of a volcanoclastic paleosol interval: implications for early Pleistocene stratigraphy and paleoclimate record, Oldavai Gorge, Tanzania: *Journal of Sedimentary Research*, v. 7, no. 5, p. 1065-1080.
- Atun, G. and Bascetin, E., 2003, Adsorption of barium on kaolinite, illite, and montmorillonite at various ionic strengths: *Radiochimica Acta*, v. 91, p. 223-228.
- Beek, K.J. and Bramaio, D.L., 1968, Nature and geography of South American soils: *in* Fittkau, E.J, ed., *Biogeography and ecology in South America*, v. 1: The Hague, W.Junk, p. 82-112.
- Behrensmeyer, A.K., Gordon, K.D., and Yanagi, G.T., 1989, Nonhuman bone modification in Miocene fossils from Pakistan: *in* Bonnicksen, R. and Sorg, M.H., *Bone Modification: Center for the Study of the First Americans*, Orono, Maine, p. 99-120.
- Boggs, Jr., S., 1995, *Principles of Sedimentology and Stratigraphy*, 2nd edition: Prentice Hall, New Jersey, 774 p.
- Breheret, J.G., Brumsack, H.J., 2000, Barite concretions as evidence of pauses in sedimentation in the Marnes Bleues Formation of the Vocontial Basin, (SE France): *Sedimentary Geology*, v. 130, p. 205-228.
- Brenner, R.L. and Peterson, J.A., 1994, Jurassic sedimentary history of the Northwestern portion of the western interior seaway, USA: *in* Caputo, M.V., Peterson, J.A., and Franczyk, K.J., (eds.), *Mesozoic systems of the Rocky Mountain region, USA: Rocky Mountain Section, Society of Economic Paleontologists and Mineralogists, Special Publication*, pp. 217-232.
- Calvo, J.P., M.M Blanc Valleron, J.P. Rodriguez, Arandia, J.M. Rouchy and M. E. Sanz, 1999, Authigenic clay minerals in continental evaporitic environments: *Special Publications of the International Association of Sedimentologists*, v. 27, p 129-151.

- Chamley, H., 1989, *Clay Sedimentology*: Springer-Verlag, New York, 623 p.
- Christiansen, E.H., Kowallis, B.J., and Barton, M.D., 1994, Temporal and spatial distribution of volcanic ash in Mesozoic rocks of the Western Interior: an alternative record of Mesozoic magmatism: *in* Caputo, M.V., Peterson, J.A., and Franczyk, K.J., eds. *Mesozoic systems of the Rocky Mountain region, USA*: Rocky Mountain Section SEPM, Denver, p. 73-94.
- Collins, M.E. and Kuehl, R.J., 2001, Organic matter accumulation and organic soils: *in* Richardson, J.L. and Vepraskas, M.J., eds., *Wetland Soils: genesis, hydrology, landscapes and classification*: Lewis Publishers, New York, p. 137-162.
- Collinson, J.D., 1996, Alluvial sediments, *in* Reading, H.G., ed., *Sedimentary Environments; processes, facies, and stratigraphy*, 3rd edition: Blackwell Science, London, p. 37-82.
- Craft, C.B., 2001, Biology of wetland soils: *in* Richardson, J.L. and Vepraskas, M.J., eds., *Wetland Soils: genesis, hydrology, landscapes and classification*: Lewis Publishers, New York, p. 107-135.
- Davies-Vollum, K.S. and Kraus, M.J., 2001, A relationship between alluvial backswamps and avulsion cycles: an example from the Willwood Formation of the Bighorn Basin, Wyoming: *Sedimentary Geology*, v. 140, p. 235-249.
- DeCelles, P.G., 2004, Late Jurassic to Eocene evolution of the Cordilleran thrust belt and Foreland basin system, western U.S.A.: *American Journal of Science*, v. 304, p. 105-168.
- Demko, T.M. and Parrish, J.T., 1998, Paleoclimatic setting of the Upper Jurassic Morrison Formation: *Modern Geology*, v. 22, p. 283-296.
- Drever, J.I., 1973. The preparation of oriented clay mineral specimens for X-ray Diffraction analysis by a filter-membrane peel technique. *American Mineralogist*, 58, pp. 553-554.
- Drits, V.A., Eberl, D.D., and Środoń, 1998, XRD measurement of mean thickness distribution and strain for illite and illite-smectite crystallites by the Bertaut-Warren-Averbach technique, *Clays and Clay Minerals*, v. 46, no. 1, p. 38-50.
- Drits, V. A., B.A. Sakharov, H. Lindgreen, and A. Salyn, 1997, Sequential structure transformation of illite-smectite-vermiculite during diagenesis of Upper Jurassic shales from the North Sea and Denmark, *Clay Mineralogy*, v. 32, p 351-371.

- Dunagan, S.P., 2000, Lacustrine carbonates of the Morrison Formation (Upper Jurassic, Western Interior), East-central Colorado, U.S.A.: *in* Gierlowski-Kordesch, E.H. and Kelts, K.R. eds.: Lake basins through space and time: AAPG Studies in Geology, v. 46, p. 181-188.
- Dunagan, S.P. and Turner, C.E., 2004, Regional paleohydrologic and paleoclimatic settings of wetland/lacustrine depositional systems in the Morrison Formation (Upper Jurassic), Western Interior, USA: *Sedimentary Geology*, v. 167, p. 269-296.
- Eberl, D.D., 2003, User's Guide to RockJock – A Program for Determining Quantitative Mineralogy from Powder X-ray Diffraction Data: U.S. Geological Survey Open-File Report 03-78, Boulder, Colorado, 45 p.
- English, P.M., 2001, Formation of analcime and moganite at Lake Lewis, central Australia: significance of groundwater evolution in diagenesis: *Sedimentary Geology*, v. 143, p. 219-244.
- Furher, L.C., 1970, Petrology and stratigraphy of nonmarine Upper Jurassic-Lower Cretaceous rocks of western Wyoming and southeastern Idaho: *American Association of Petroleum Geologists Bulletin*, v. 54, no. 12, p. 2282-2302.
- Gottardi, G. and Galli, E., 1985, *Natural Zeolites*: Springer-Verlag, New York, 409 p.
- Gran, K.B. and Montgomery, 2005, Spatial and temporal patterns in fluvial recovery following volcanic eruptions: channel response to basin-wide sediment loading at Mount Pinatubo, Philippines: *Geological Society of America Bulletin*, v. 117, no. 1-2, p. 195-211.
- Hanor, J.S., 2000. Barite-celestine geochemistry and environments of formation, *in* Alpers, C.N., Jambor, J.L., and Nordstrom, D.K., eds., *Sulfate Minerals: crystallography, geochemistry, and environmental significance: Reviews in Mineralogy and Geochemistry*: Washington D.C., Mineralogical Society of America, p. 193-275.
- Hasiotis, S.T., 2000, The invertebrate invasion and evolution of Mesozoic soil ecosystems: the ichnofossil record of ecological innovations: *in* Gastaldo, R. and Dimichele, W., eds., *Phanerozoic Terrestrial Ecosystems*, Paleontological Society Short Course, v. 6, p. 141-169.
- Hasiotis, S.T., 2002, *Continental Trace Fossil Atlas*. SEPM, Short Course Notes Number 51, Tulsa, Oklahoma, 132 p.

- Hasiotis, S.T., 2004, Reconnaissance of Upper Jurassic Morrison Formation ichnofossils, Rocky Mountain Region, USA: paleoenvironmental, stratigraphic, and paleoclimatic significance of terrestrial and freshwater ichnocoenoses: *Sedimentary Geology*, v. 167, p. 177-268.
- Hasiotis, S.T. and Demko, T.M., 1996, Terrestrial and freshwater trace fossils, Upper Jurassic Morrison Formation, Colorado Plateau: *in* Morales, M., ed., *The Continental Jurassic: Museum of Northern Arizona Bulletin* 60.
- Hasiotis, S. T., Wellner, R. W., Martin, A., and Demko, T. M., 2004, Vertebrate burrows from Triassic and Jurassic continental deposits of North America and Antarctica: their paleoenvironmental and paleoecological significance. *Ichnos*, v. 11, p. 103-124.
- Hay, R.L., 1970, Silicate reactions in three lithofacies of a semi-arid basin, Olduvai Gorge, Tanzania: *Mineralogical Society of America, Special Paper* 3, p. 237-255.
- Hillier, S., 1995, Erosion, sedimentation, and sedimentary origin of clays: *in* Velde, B., ed., *Origin and Mineralogy of Clays: clays and the environment: Springer-Verlag New York*, p. 162-219.
- Hurt, G.W. and Carlisle, V.W., 2001, Delineating hydric soils: *in* Richardson, J.L. and Vepraskas, M.J., eds., *Wetland Soils: genesis, hydrology, landscapes and classification: Lewis Publishers, New York*, p.183-206.
- Irving, W.N., Jopling, A.V., and Kritsch-Armstrong, I., 1989, Studies of bone technology and taphonomy, Old Crow Basin, Yukon Territory: *in* Bonnicksen, R. and Sorg, M.H., *Bone Modification: Center for the Study of the First Americans, Orono, Maine*, p. 347-380.
- Johnson, J, 1991, Stratigraphy, Sedimentology, and depositional environments of the Upper Jurassic Morrison Formation, Colorado Front Range: *Dissertation, University of Nebraska, Lincoln*, pp. 171.
- Kataoka, K., 2005, Distal fluvial-lacustrine volcanoclastic resedimentation in response to an explosive silicic eruption: the Pliocene Mushono tephra bed, central Japan: *Geological Society of America Bulletin*, v. 117, no. 1-2, p. 3-17.
- Kraus, M.J., 1997, Lower Eocene alluvial paleosols: pedogenic development, stratigraphic relationships, and paleosol/landscape associations: *Palaeogeography, Palaeoclimatology, Palaeoecology*, v. 129, p. 387-406.

- Kraus, M.J., 1999, Paleosols in clastic sedimentary rocks: their geologic applications; *Earth-Science Reviews*, v. 47, p. 41-70.
- Kraus, M.J., 2002, Basin-scale changes in floodplain paleosols: implications for interpreting alluvial architecture: *Journal of Sedimentary Research*, v. 72, no. 4, p. 500-509.
- Kraus, M.J. and Gwinn, B., 1997, Facies and facies architecture of Paleogene floodplain deposits, Willwood Formation, Bighorn Basin, Wyoming, USA: *Sedimentary Geology*, v. 114, p. 33-54.
- Kuenzi, W.D., Horst, O.H., and McGehee, R.V., 1979, Effect of volcanic activity on fluvial-deltaic sedimentation in a modern arc-trench gap, southwestern Guatemala: *Geological Society of America Bulletin*, Part 1, v. 90, p. 827-838.
- Lawton, T.F. 1994, Tectonic setting of Mesozoic sedimentary basins, Rocky Mountain region, United States: *in* Caputo, M.V., Peterson, J.A., and Franczyk, K.J., (eds.), *Mesozoic systems of the Rocky Mountain region, USA: Rocky Mountain Section, Society of Economic Paleontologists and Mineralogists, Special Publication*, p. 1-25.
- Litwin, R.J., Turner, C.E., and Peterson, F., 1998, Palynological evidence on the age of the Morrison Formation, Western Interior U.S.; *Modern Geology*, v. 22, p.297-319.
- Luo, Z. and Wible, J.R., 2005, A Late Jurassic digging mammal and early mammalian diversification: *Science*, v. 308, p. 103-107.
- Major, J.J., Pierson, T.C., and Costa, J.E., 2000, Sediment yield following severe volcanic disturbance—a two-decade perspective from Mount St. Helens: *Geology*, v. 28, no. 9, p. 819-822.
- Martin, R.E., 1999, *Taphonomy: a process approach*: Cambridge University Press, Cambridge, 508 p.
- Makaske, B., 2001, Anastomosing rivers: a review of their classification, origin, and sedimentary products: *Earth Sciences Reviews*, v. 53, p. 149-196.
- Meunier, A. and Velde, B., 2004, *Ilite: origins, evolution, and metamorphism* Springer Verlag, New York, 286 p.
- Moore, R.C. and Reynolds, D.M., 1997. *X-ray diffraction and the identification and analysis of clay minerals*, Oxford University Press, pp. 378.

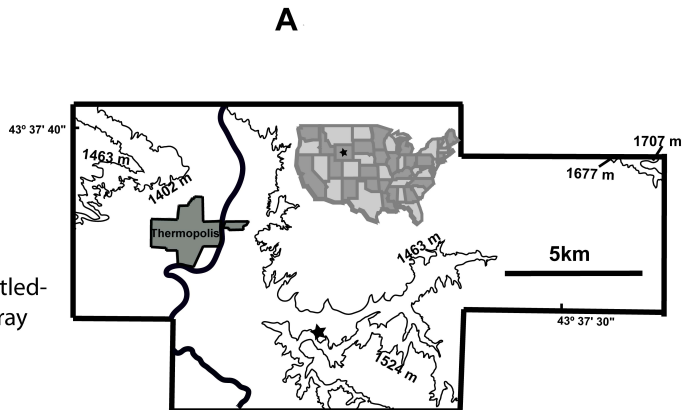
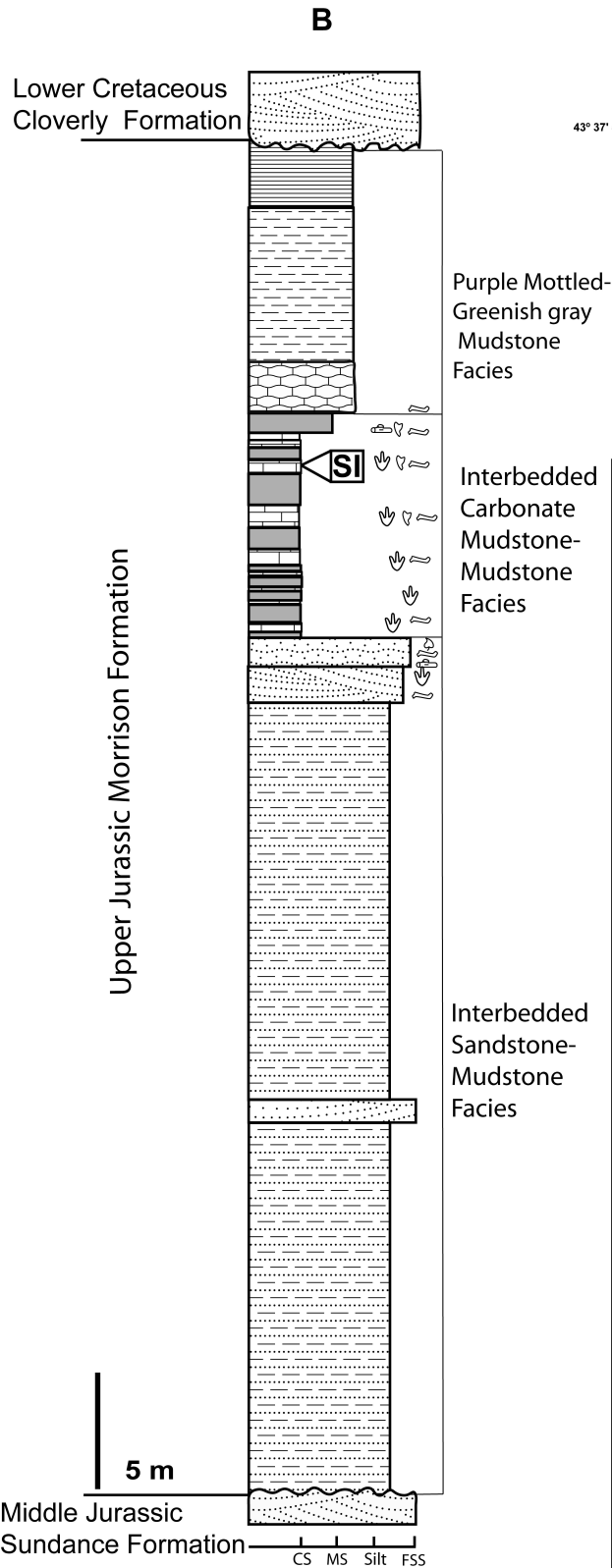
- Mirsky, A., 1962, Stratigraphy of non-marine Upper Jurassic and Lower Cretaceous rocks, southern Big Horn Mountains, Wyoming: *Bulletin of the American Association of Petroleum Geologists*, v. 46, no. 9, p. 1653-1680.
- Parrish, J.T., Peterson, F., and Turner, C.E., 2004, Jurassic “savannah” – plant taphonomy and climate of the Morrison Formation (Upper Jurassic, Western USA): *Sedimentary Geology*, v. 167, p. 137-162.
- Peterson, F. 1994, Sand dunes, sabkhas, streams, and shallow seas: Jurassic Paleogeography in the southern part of the western interior basin: *in* Caputo, M.V., Peterson, J.A., and Franczyk, K.J., eds. *Mesozoic systems of the Rocky Mountain region, USA: Rocky Mountain Section SEPM, Denver*, p. 233-272.
- Peterson, J.A., 1972, Jurassic System: *in* Mallory, W.W. Ed. *Geologic Atlas of the Rocky Mountain Region: Rocky Mountain Association of Geologists, Denver, Colorado*, pp.331.
- Pipujol, M.D. and Buurman, P., 1994, The distinction between ground-water gley and surface-water gley phenomena in Tertiary paleosols of the Ebro basin, NE Spain: *Palaeogeography, Palaeoclimatology, Palaeoecology*, v. 110, p. 103-113.
- Platt, N.H., 1989, Lacustrine carbonates and pedogenesis: sedimentology and origin of palustrine deposits from the Early Cretaceous Rupelo Formation, W. Cameros Basin, N. Spain. *Sedimentology*, 36, pp 665-684.
- Platt, S.G., Rainwater, T.R., and Brewer, S.W., 2004, Aspects of the burrowing ecology of nine-banded armadillos in northern Belize: *Mammalian Biology*, v. 69, no. 4, p. 217-224.
- Rees, P.M., Noto, C.R., Parrish, N.J., and Parrish, J.T., 2004, Late Jurassic climates, vegetation, and dinosaur distributions: *Journal of Geology*, v. 112, p. 643-653.
- Renaut, R.W., 1993, Zeolitic diagenesis of late Quaternary fluvio-lacustrine sediments and associated calcretes formation in the Lake Borgoria Basin, Kenya Rift Valley: *Sedimentology*, v. 40, p. 271-301.
- Retallack, G.J., 1997, *A Colour Guide to Paleosols*: John Wiley and Sons, New York, 175 p.

- Richardson, J.L., Arndt, J.L., and Montgomery, J.A., 2001, Hydrology of wetland and related soils: *in* Richardson, J.L. and Vepraskas, M.J., eds., *Wetland Soils: genesis, hydrology, landscapes and classification*: Lewis Publishers, New York, p. 35-84.
- Righi D. and Meunier, A., 1995, Origin of clays by rock weathering and soil formation: *in* Velde, B., *Origin and Mineralogy of Clays*: Springer-Verlag, Berlin, 334 p.
- Ryan, P.C., and Hillier, S., 2002, Berthierine/chamosite, corrensite, and discrete chlorite from evolved verdine and evaporite-associated facies in the Jurassic Sundance Formation, Wyoming: *American Mineralogist*, v. 87, no. 11-12, p. 1607-1615.
- Santos, E.S., and Peterson, C.E., 1986, Tectonic setting of the San Juan Basin in the Jurassic: *in* Turner-Peterson, C.E., Santos E.S., Fishman, N.S., eds., *A Basin Analysis Case Study: the Morrison Formation, Grants Uranium Region, New Mexico*: American Association of Petroleum Geologists Studies in Geology # 22, pp 27-33.
- Seal, R.R., Alpers, C.N., and Rye, R.O., 2000, Stable isotope systematics of sulfate minerals: *in* Alpers, C.N., Jambor, J.L., and Nordstrom, D.K., eds., *Sulfate minerals: crystallography, geochemistry, and environmental significance: Reviews in mineralogy and geochemistry*, Mineralogical Society of America, Washington, D.C., p. 541-602.
- Slingerland, R. and Smith, N.D., 2004, River avulsions and their deposits: *Annual Reviews of Earth and Planetary Science*, v. 32, p. 257-285.
- Smith, G.A., 1988, Sedimentology of proximal to distal volcanoclastics dispersed across an active foldbelt: Ellensburg Formation (late Miocene), central Washington: *Sedimentology*, v. 35, 953-977.
- Stokes, W.L., 1944, Morrison Formation and related deposits in and adjacent to the Colorado Plateau: *Bulletin of the Geological Society of America*, v. 55, p. 951-992.
- Surdam, R.C. and Eugster, H.P., 1976, Mineral reactions in the sedimentary deposits of the Lake Magadi region, Kenya: *Geological Society of America Bulletin*, v. 87, p. 1739-1752.
- Suttner, Lee. 1969, Stratigraphic and petrographic analysis of Upper Jurassic Lower Cretaceous Morrison and Kootenai Formations, Southwest Montana: *American Association of Petroleum Geologists Bulletin*, v. 53, no. 7, p 1391-1410.

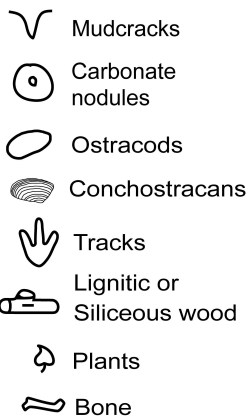
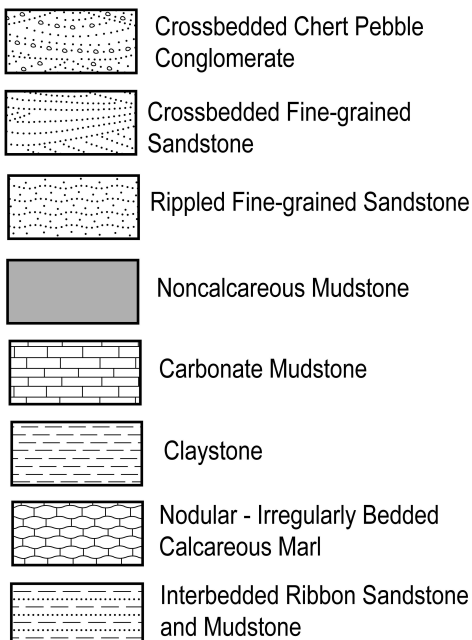
- Talbot, M.R. and Allen, P.A., 1996, Lakes, *in* Reading, H.G., ed., Sedimentary Environments; processes, facies, and stratigraphy, 3rd edition: Blackwell Science, London, p. 83-124.
- Taylor, M.W. and Surdam, R.C., 1981, Zeolite reactions in the tuffaceous sediments at Teels Marsh, Nevada: *Clays and Clay Minerals*, v. 25, no. 5, p. 341-352.
- Tidwell, W.D., 1990, Preliminary report on the megafossil flora of the Upper Jurassic Morrison Formation: *Hunteria*, v. 2, no. 8, 12 p.
- Turner, C.E. and Peterson, F., 1999, Biostratigraphy of dinosaurs in the Upper Jurassic Morrison Formation of the Western Interior, U.S.A.: *in* Gillette, D.D., ed., Vertebrate Paleontology in Utah: Utah Geological Survey, v. 99-1, p. 77-114.
- Utada, M., 1988, Occurrence and genesis of hydrothermal zeolites and related minerals from the Kuroko-type mineralization areas in Japan: *in* Kallo, D. and Sherry, H.S., eds., Occurrence, Properties, and Utilization of Natural Zeolites, H. Stillman Publishers, Inc., Boca Raton, 857 p.
- Vepraskas, M.J., 2001, Morphological features of seasonally reduced soils: *in* Richardson, J.L. and Vepraskas, M.J., eds., Wetland Soils: genesis, hydrology, landscapes and classification: Lewis Publishers, New York, 163-206.
- Vespraskas, M.J. and Faulkner, S.P., 2001, Redox chemistry of hydric soils: *in* Richardson, J.L. and Vepraskas, M.J., eds., Wetland Soils: genesis, hydrology, landscapes and classification: Lewis Publishers, New York, p. 85-105.
- Walker, R.G. and Cant, D.J., 1984, Sandy fluvial systems, *in* Walker, R.G. ed., Facies Models, 2nd edition: Geological Association of Canada, St. John's, Newfoundland, Canada, p. 71-89.
- Way, J.N., Malley, P.J., Furer, L.C., Suttner, L.J., Kvale, E.P., and Meyers, J.H., 1994, Correlations of the Upper Jurassic-Lower Cretaceous nonmarine and transitional Rocks in the northern Rocky Mountain foreland: *in* Caputo, M.V., Peterson, J.A., and Franczyk, K.J., eds., Mesozoic systems of the Rocky Mountain region, USA: Rocky Mountain Section SEPM, Denver, p. 351-364.

CHAPTER 4. CONCLUSIONS

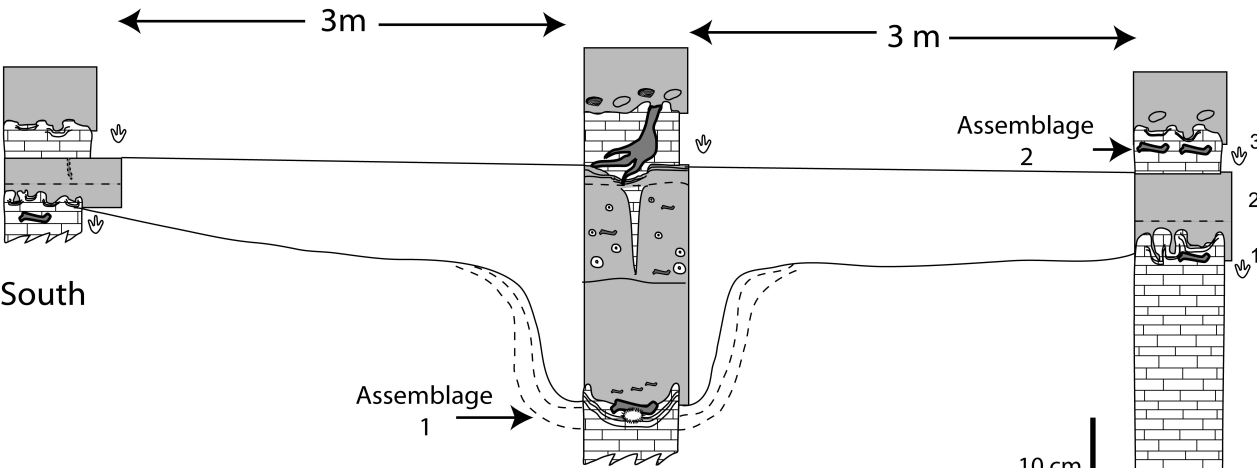
Continental deposits tend to be extremely laterally variable over short distances, frustrating efforts to make consistent paleoenvironmental interpretations. Results of this study show that combining modern and traditional geological and paleontological data using traditional and modern methods is a valuable way to approach paleoenvironmental and taphonomic studies. Traditional methods alone are not adequate enough to provide sufficient chronological constraints in homogenous units when evaluating the degree of time averaging of a fossil assemblage in continental deposits. The use of three-dimensional maps in taphonomic studies offers researchers a better tool to evaluate spatial relationships between fossil elements and geological data. By synthesizing geochemical, sedimentological, and paleontological data complex paleoenvironmental patterns can be better evaluated. The combination of traditional and modern paleontological field methods improves our ability to integrate taphonomic and paleoenvironmental information in complex assemblages and enhance our understanding of ancient paleoecology.








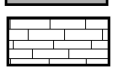





Lithostratigraphic Key

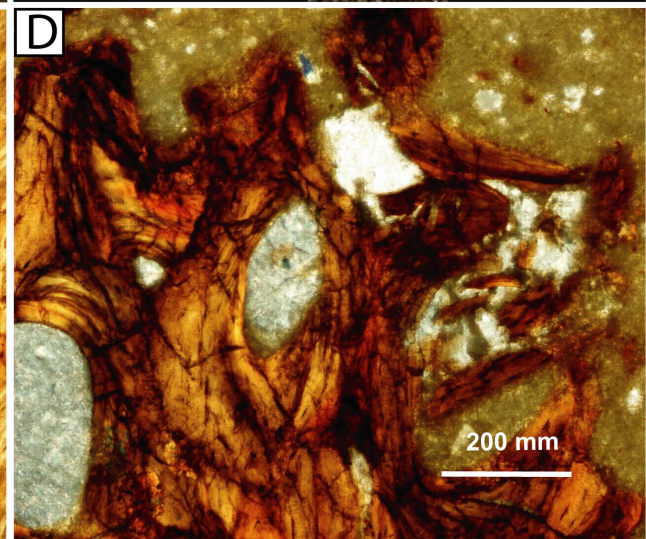
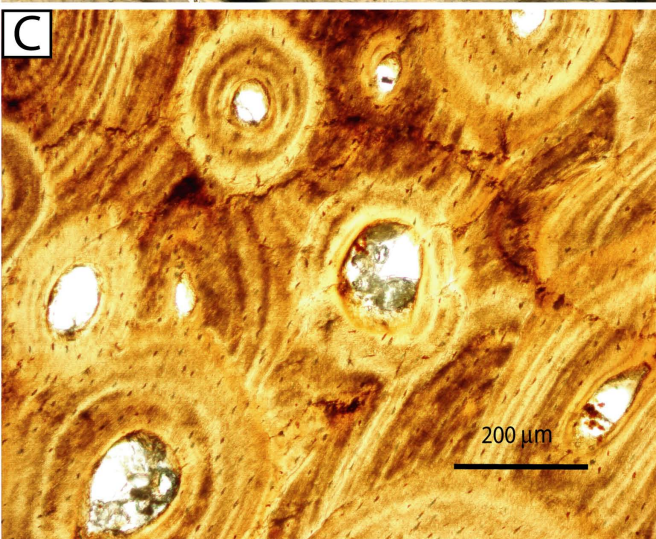
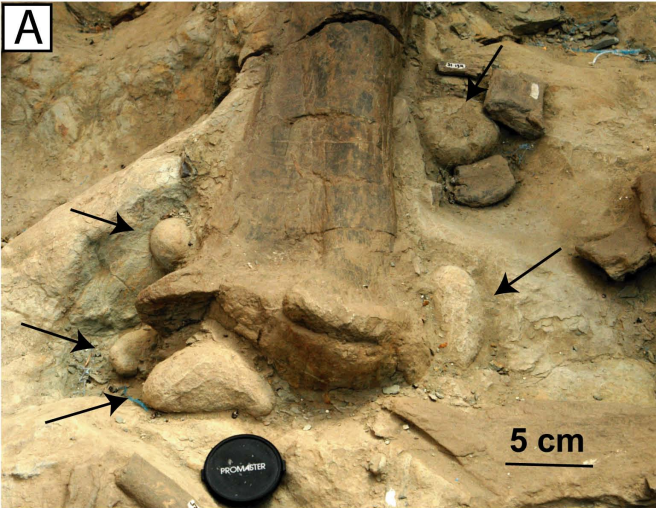


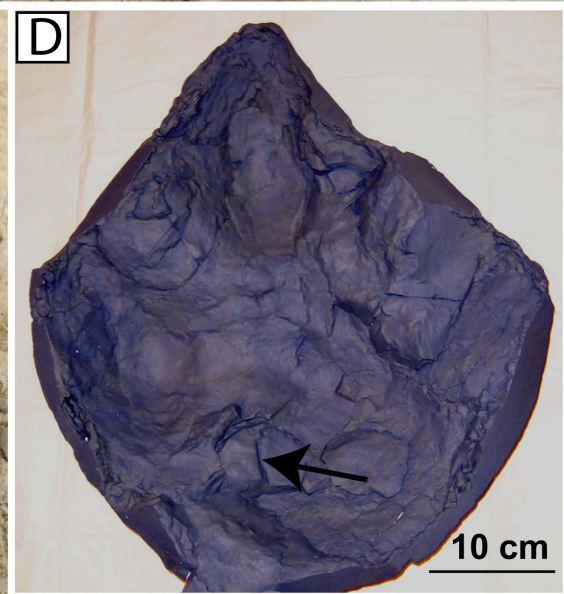
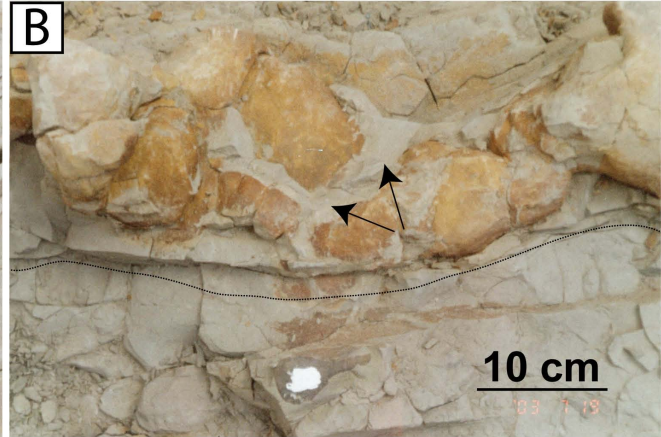
High resolution stratigraphic sections along dinosaur quarry

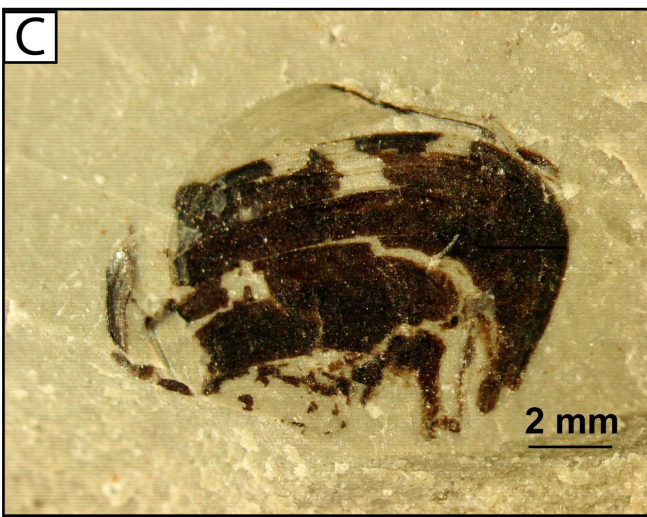
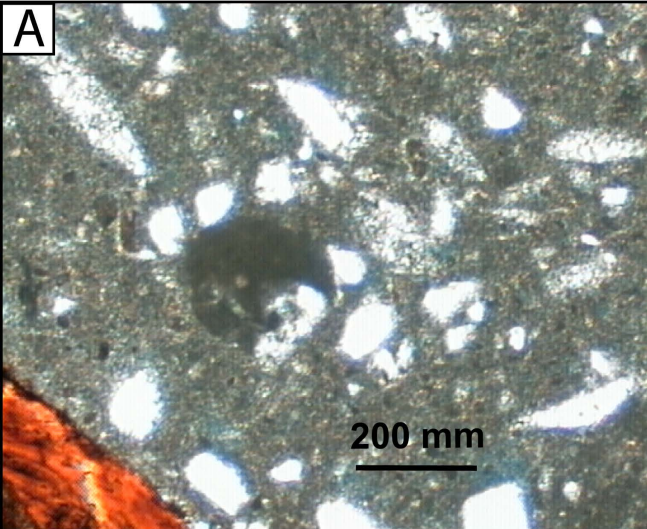


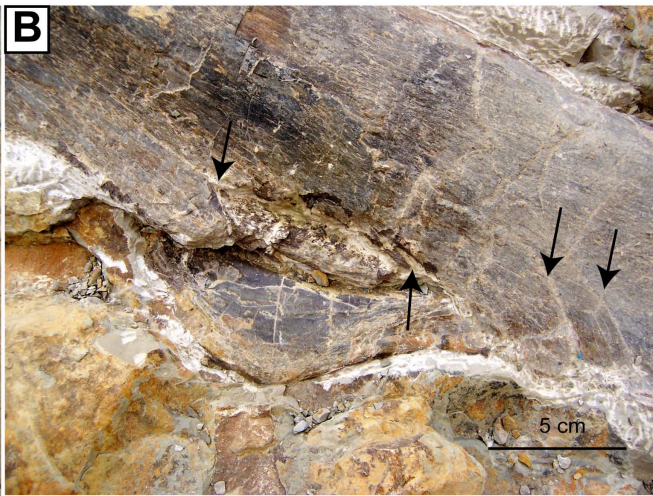
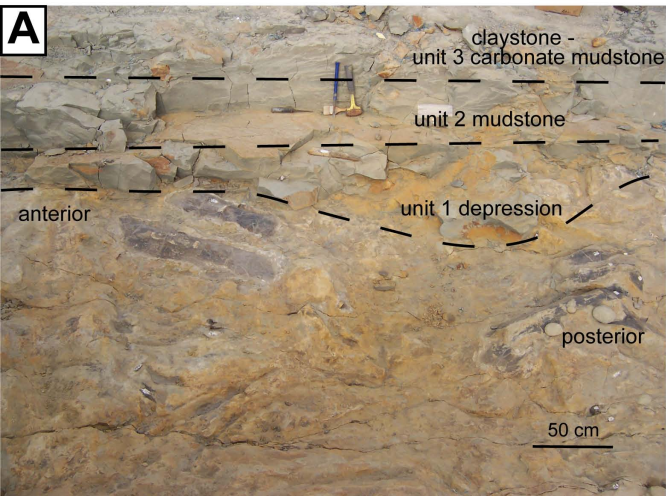
KEY

	Mudcracks		Tracks		Noncalcareous Mudstone
	Carbonate nodules		Lignitic or Siliceous wood		Carbonate Mudstone
	Ostracods		Plants		barite
	Conchostracans		Bone		

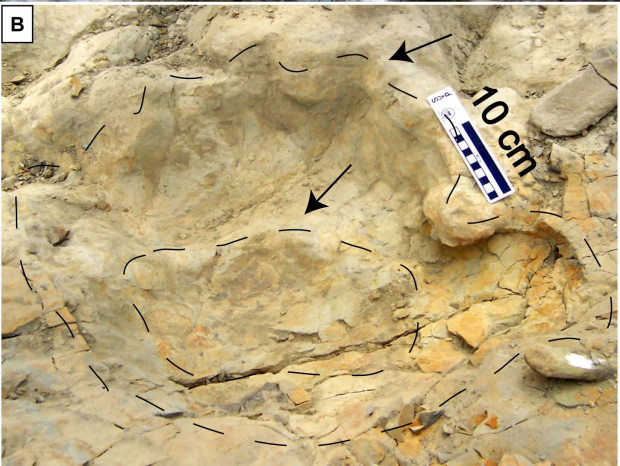


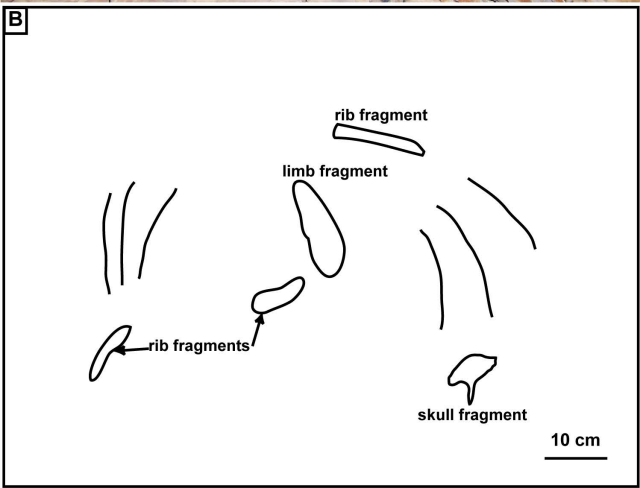
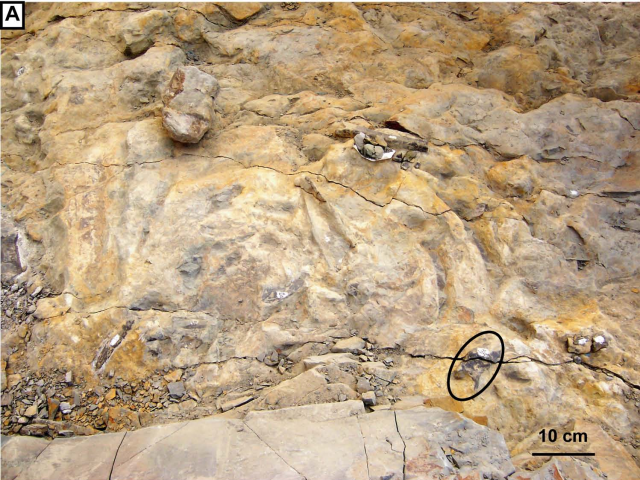


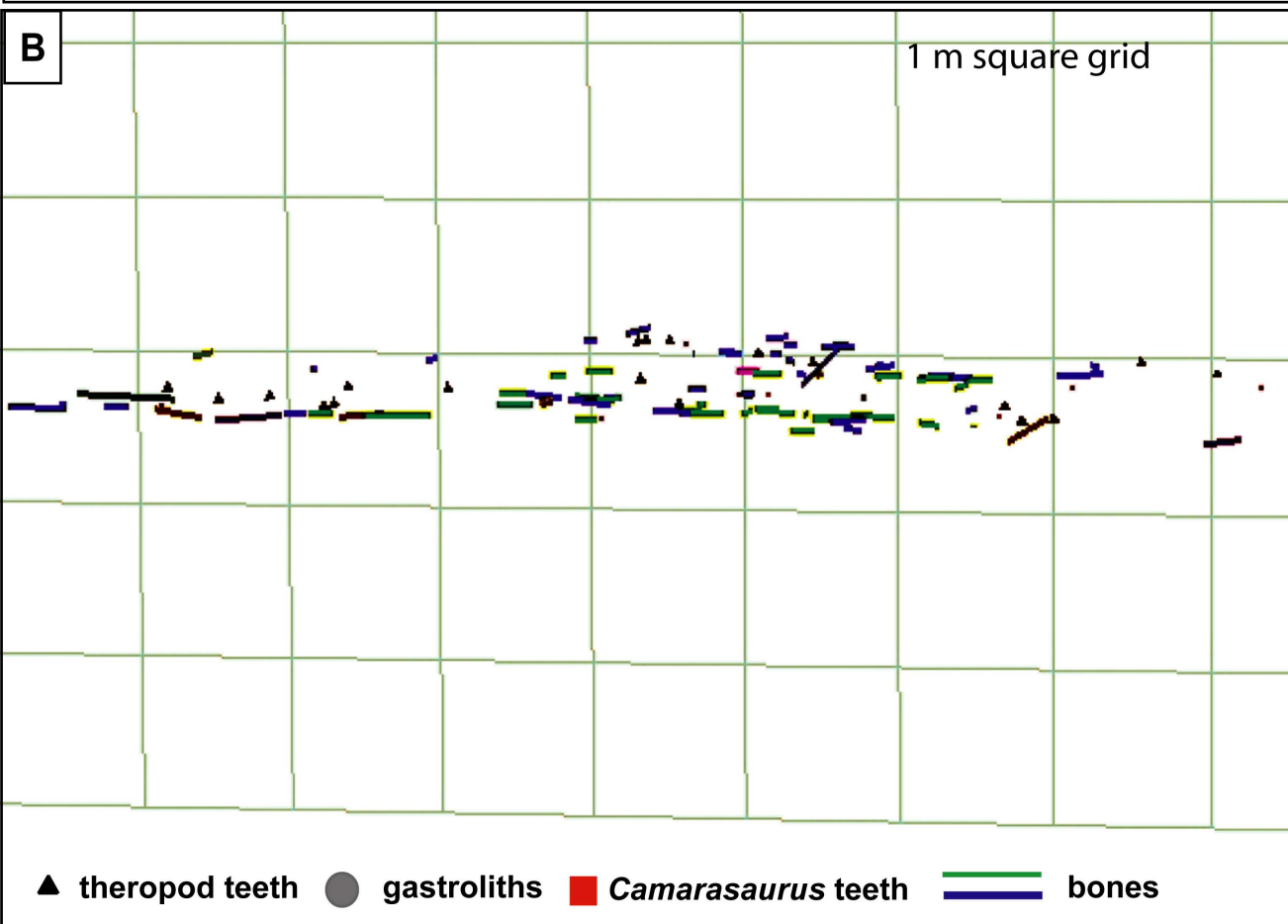
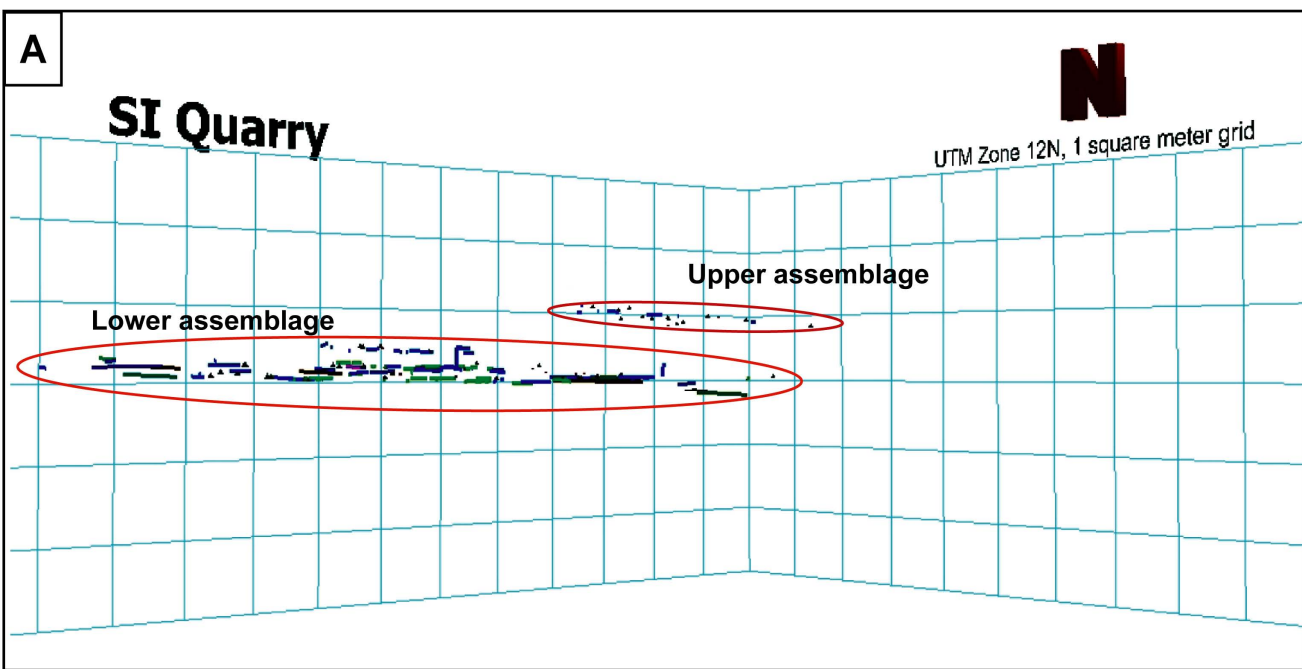


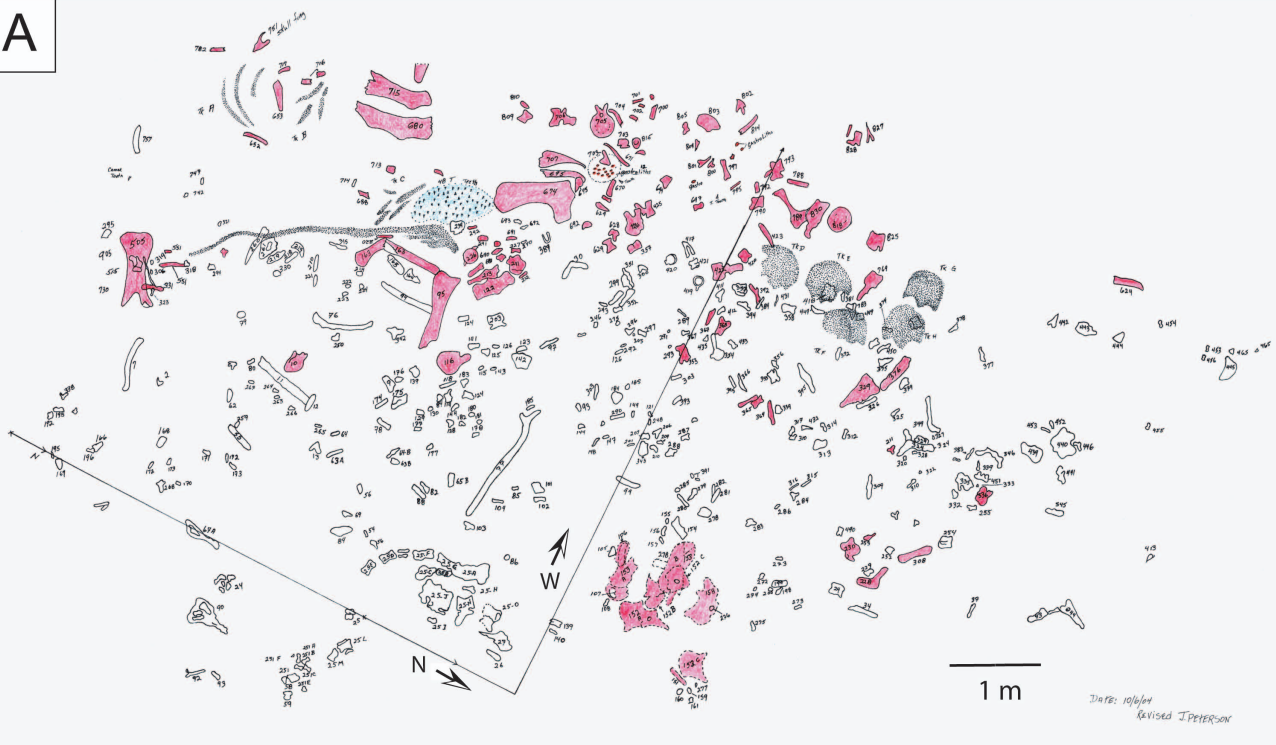
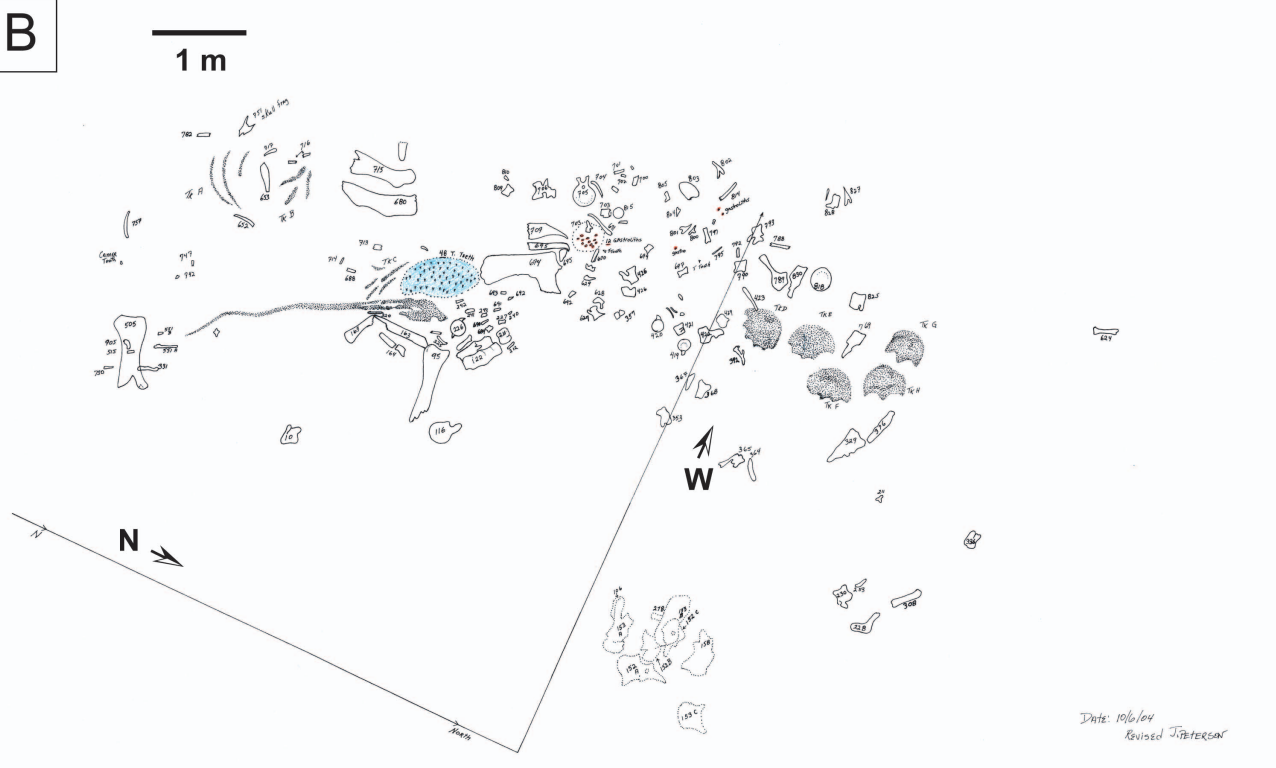


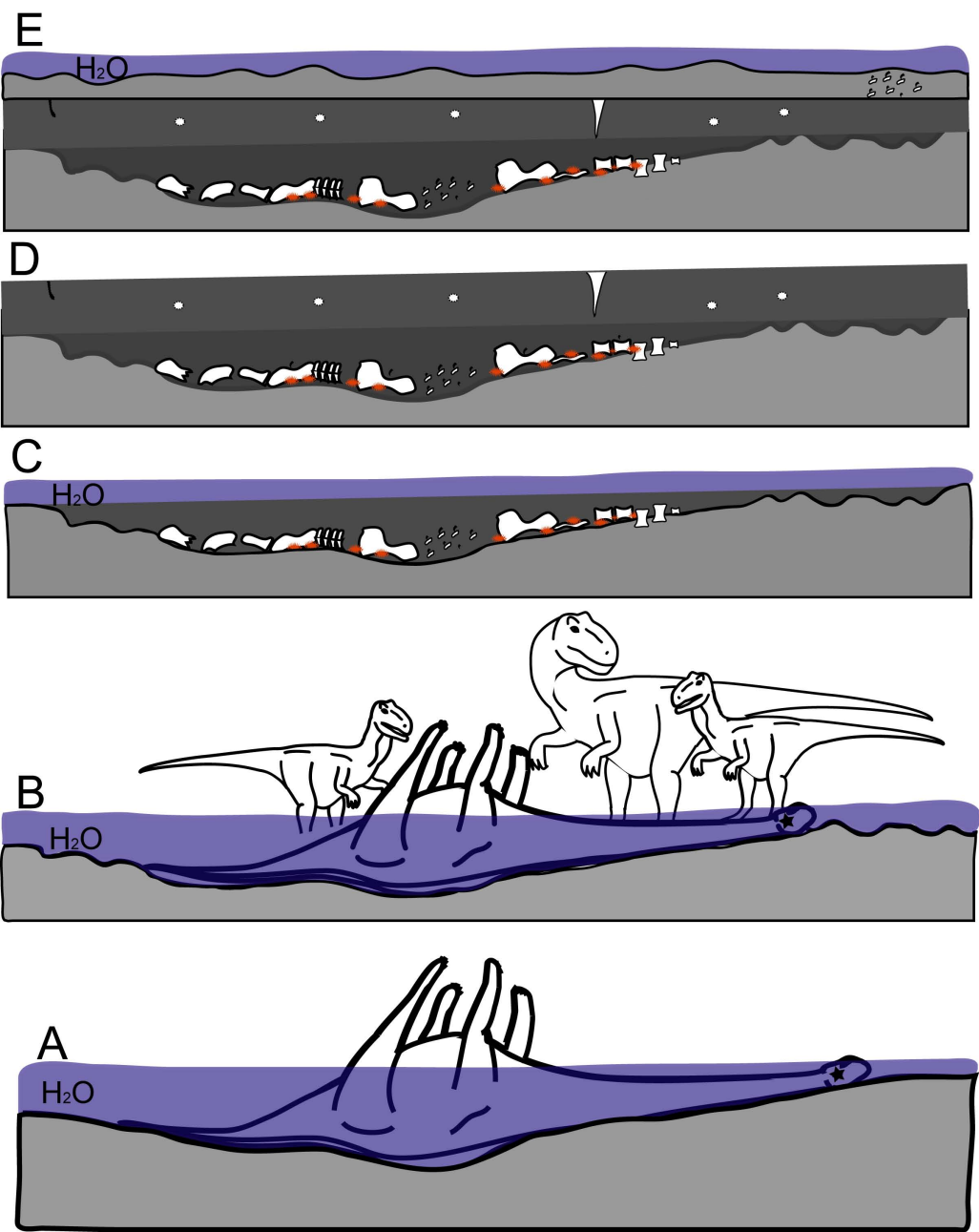




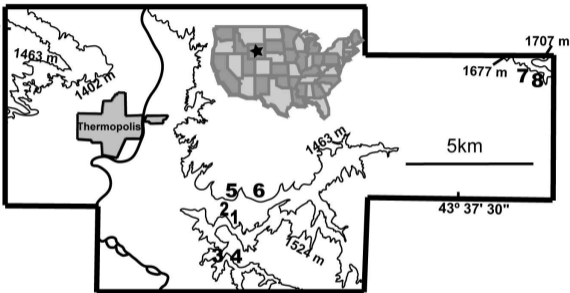


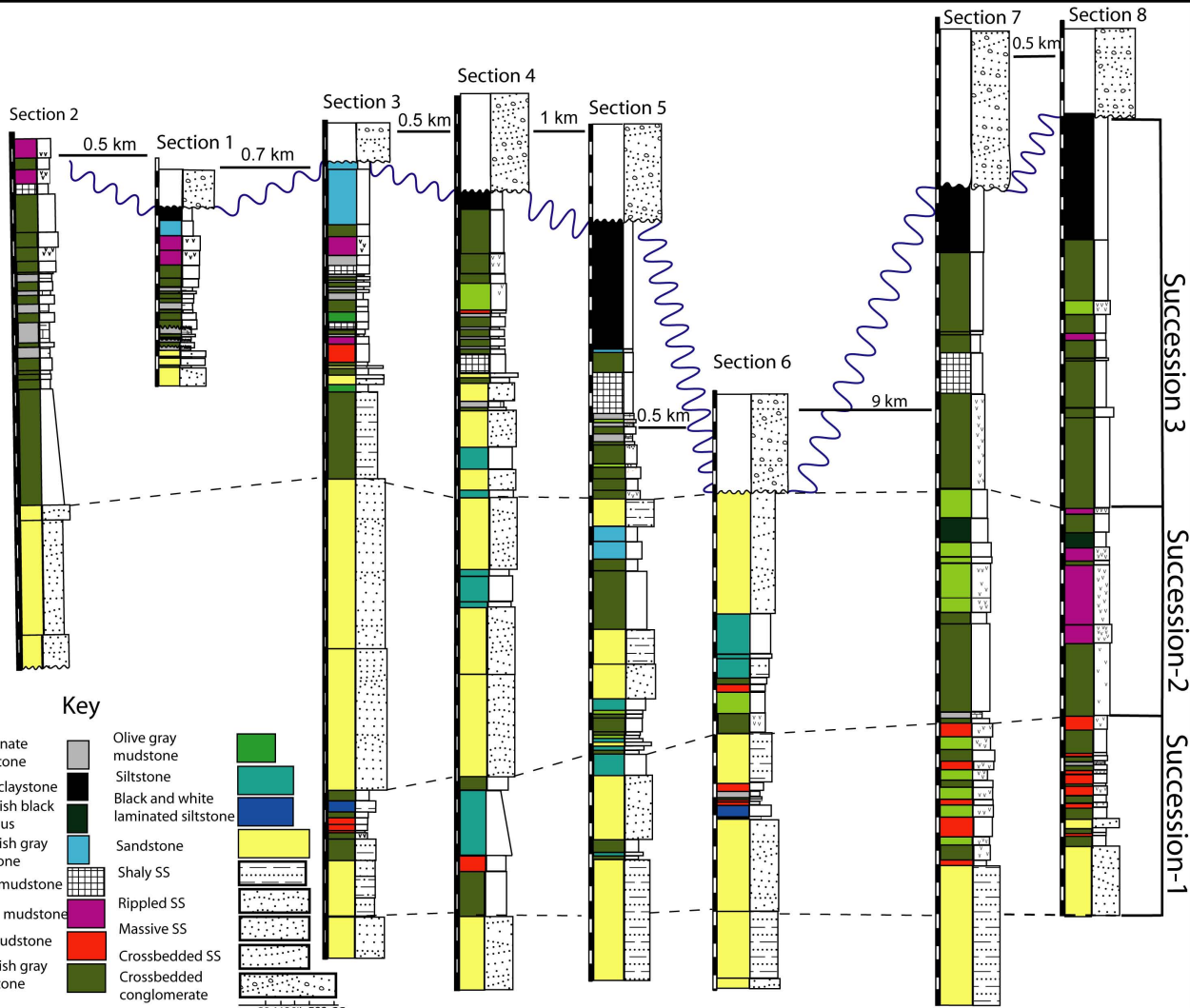


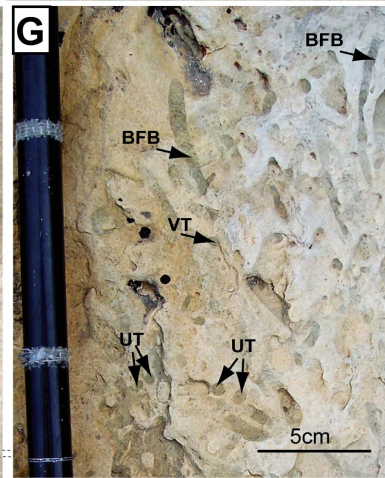
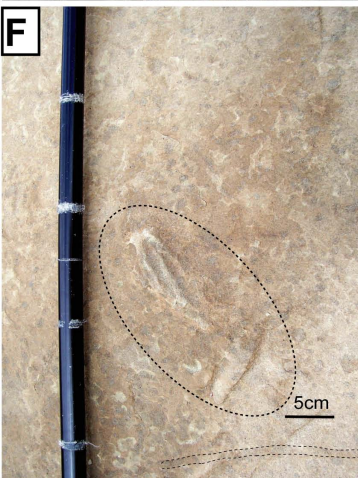
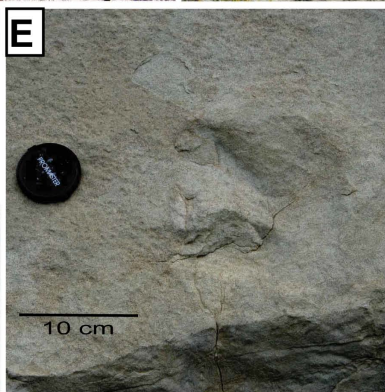
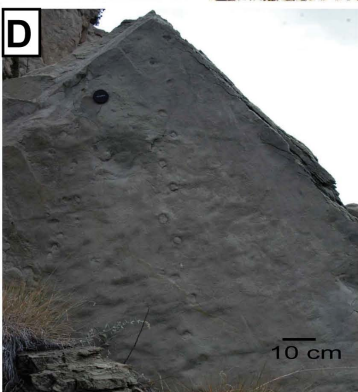
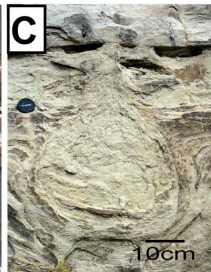
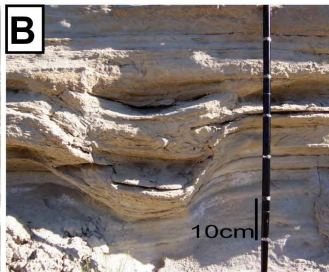
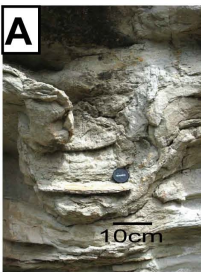
A**B**



43° 37' 40"







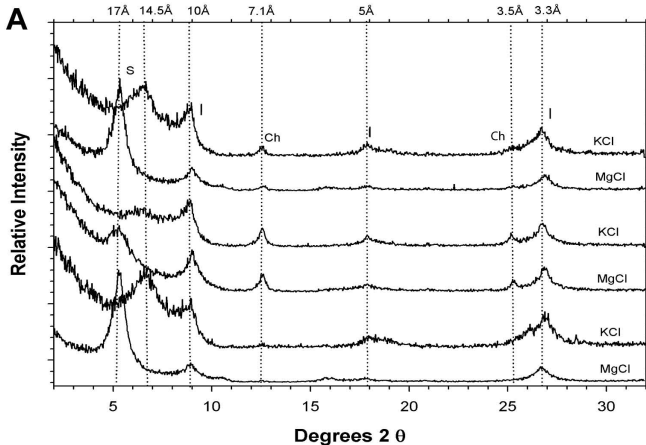
thorax

cephalon

5cm

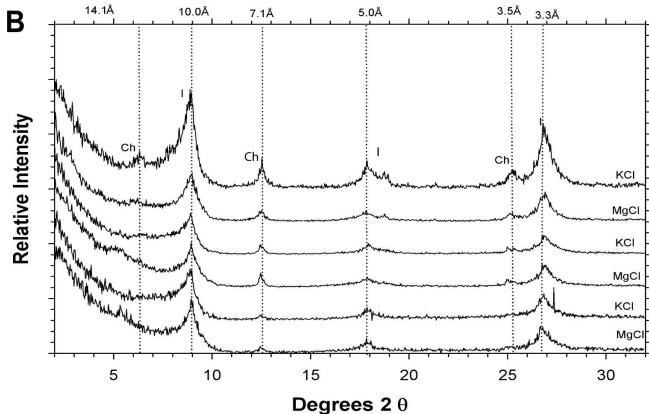
PROMASTER

Proximal Floodplain deposits

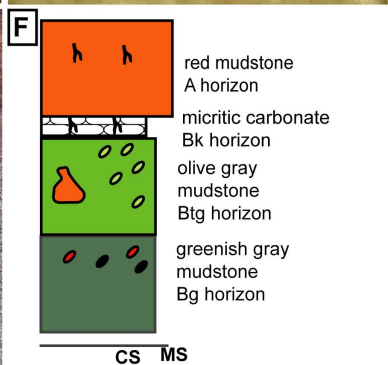
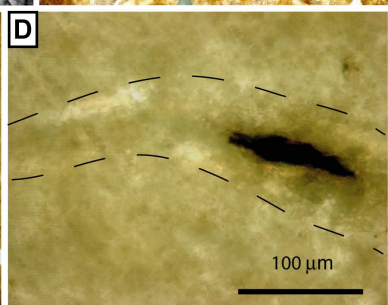
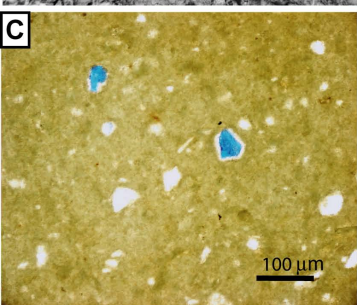
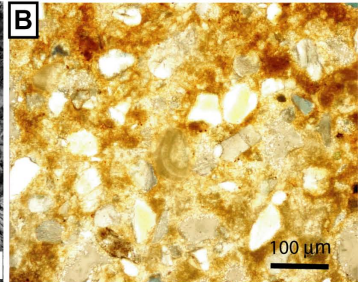
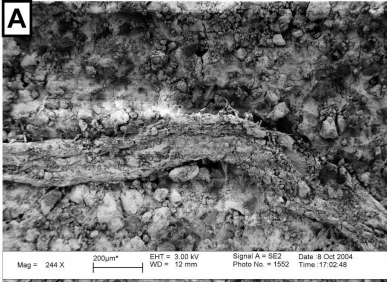


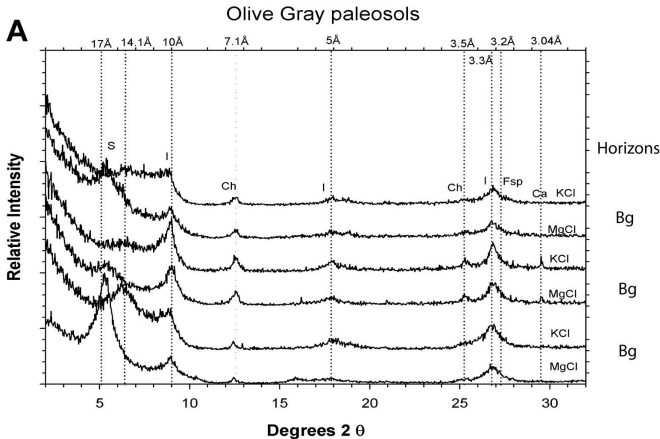
Floodplain Paleosols = siltstone - poorly developed well-drained paleosols

Well-drained paleosols

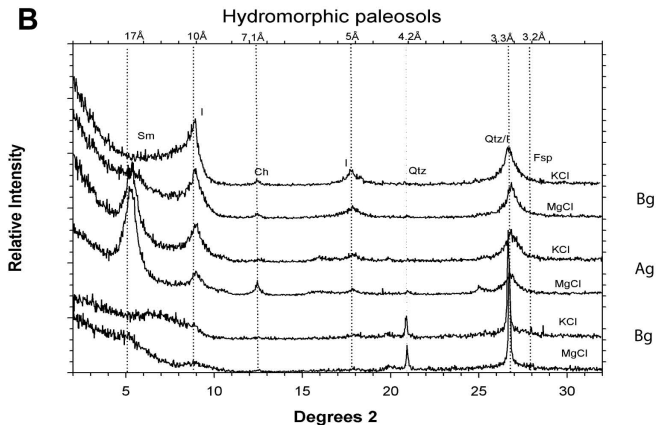


Well-drained paleosols = red mudstone; olive gray mudstone; greenish gray mudstone

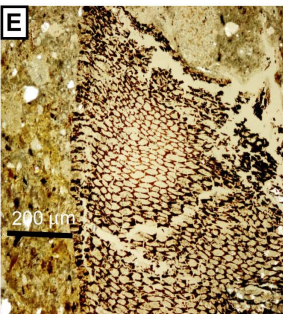
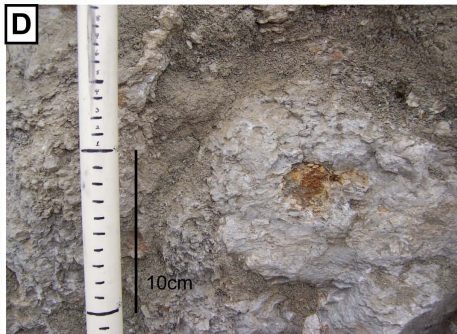
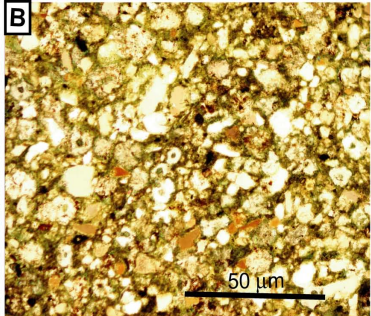
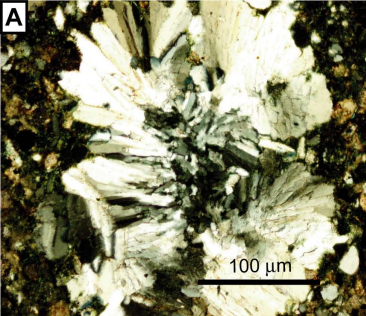




Olive gray paleosols = olive gray mudstone; light olive gray mudstone

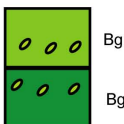


Hydromorphic paleosols = purple mudstone with greenish gray and red mottles

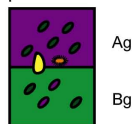


F

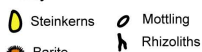
Olive gray
paleosol



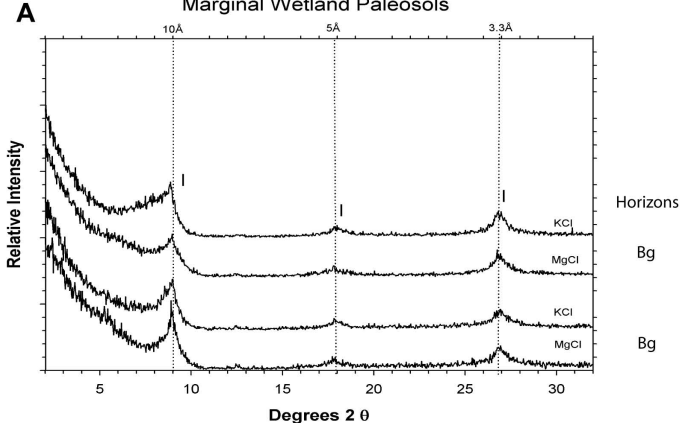
Hydromorphic
paleosol



Key



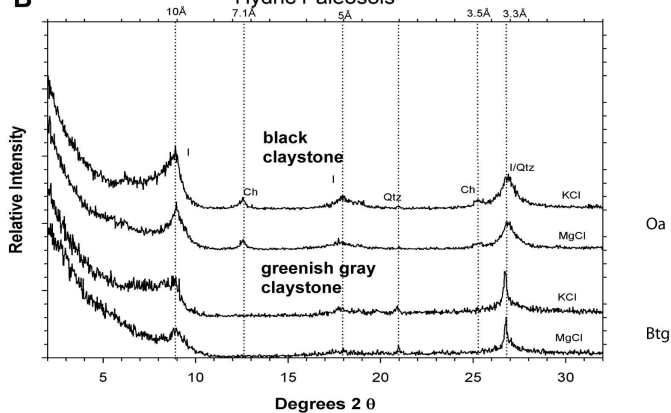
Marginal Wetland Paleosols



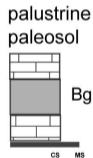
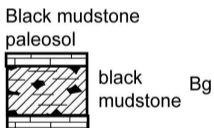
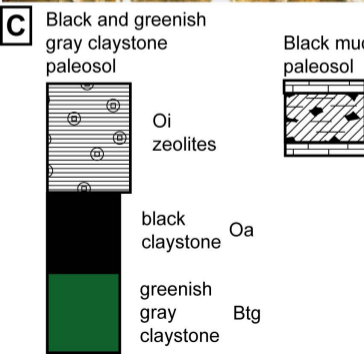
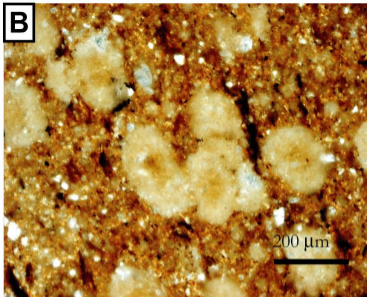
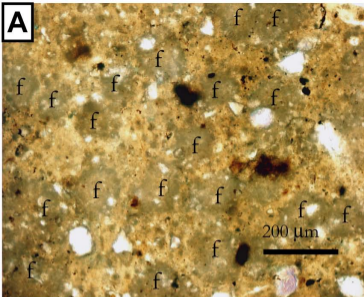
Marginal wetland paleosols = black mudstone

B

Hydric Paleosols

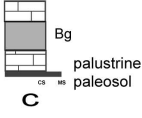
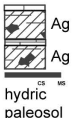
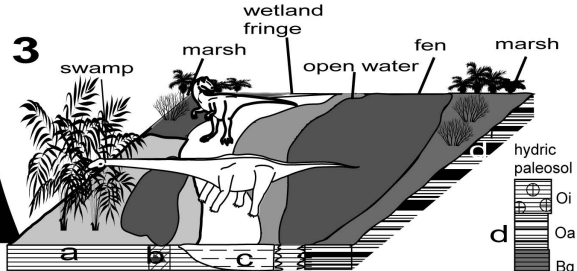


Hydric paleosols = greenish gray and black claystone



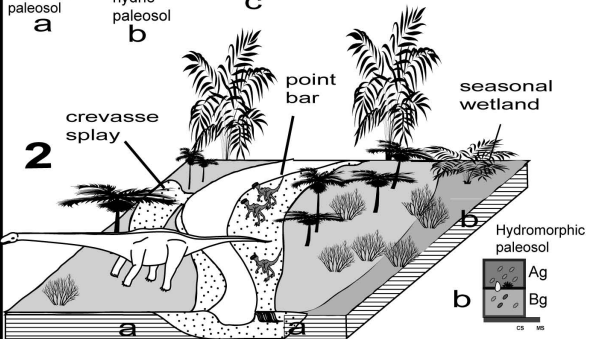
Increasing saturation and steadier sedimentation rate

3



d

2



1

